Evaluation of Tumour-Infiltrating Immune Cells and Their Prognostic Impact in Feline Oral Squamous Cell Carcinoma and Appendicular Osteosarcoma

(猫の口腔扁平上皮癌および四肢骨肉腫における腫瘍浸潤免疫細胞の評価とその予後への影響)

Joint Graduate School of Veterinary Medicine

Yamaguchi University

Arief Purwo Mihardi

September 2026

SUMMARY

Cancer is a common disease and a leading cause of death in domestic animals, including cats. Among felines, carcinomas are the most frequently diagnosed tumours, with squamous cell carcinoma being the predominant type. Although relatively rare, osteosarcoma represents the most common primary bone tumour in cats. In recent years, immune-based approaches have been increasingly explored to better understand and target tumour development and progression. A major focus has been placed on tumour-infiltrating immune cells, key tumour microenvironment components. However, their role in feline tumours, particularly oral squamous cell carcinoma and osteosarcoma, remains poorly understood and warrants further investigation.

A total of 36 feline tumour samples, comprising 20 cases of oral squamous cell carcinoma and 16 cases of osteosarcoma, were analysed immunohistochemically for $CD3^+$ T cells, $CD8^+$ T cells, $Foxp3^+$ regulatory T cells, $CD20^+$ B cells and $CD204^+$ macrophages to characterise immune cells composition. Clinicopathological features were evaluated for associations with immune cell infiltration, and survival was analysed using the Kaplan–Meier method with the log-rank test.

In feline oral squamous cell carcinoma, $CD3^+$ and $CD8^+$ T cells were frequently detected in both stromal and tumour regions, while $CD20^+$ B cells were significantly enriched in the stroma. $Foxp3^+$ Tregs and $CD204^+$ macrophages were variably present across cases. Strong positive correlations were observed among T cells, B cells, Tregs and macrophages, particularly within the stroma. Although immune cell infiltration was not directly associated with clinicopathological parameters, higher densities of stromal $CD20^+$ B cells and tumour $CD3^+$ T cells correlated with shorter progression-free intervals and tumour $CD3^+$ T cells were inversely associated with overall survival. Kaplan–Meier

analysis further demonstrated that lower stromal $CD8^+$ and tumour $CD3^+$ T cell infiltration was linked to better clinical outcomes. These findings suggest that pronounced T cell infiltration, especially of $CD3^+$ and $CD8^+$ subsets, may predict poorer prognosis in feline oral squamous cell carcinoma.

In feline osteosarcoma, the femur was the most frequently affected site, and radiographic abnormalities and lameness were observed in most cases. Lymph node and distant metastases occurred in 6.3% and 43.8% of cases, respectively, with significant associations between metastatic status and prognosis. The median overall survival time was 320 days. Immunohistochemical analysis revealed that $CD204^+$ macrophages were the most abundant immune population, followed by $CD3^+$ and $CD8^+$ T cells, $CD20^+$ B cells and $Foxp3^+$ regulatory T cells. High $CD3^+$ T cell density was significantly associated with poor prognosis, whereas $CD8^+$ T cells and $CD204^+$ macrophages showed weaker associations. Moreover, $CD3^+$ and $CD8^+$ T cell densities decreased with age, suggesting an age-related decline in immune surveillance and their higher infiltration levels were correlated with shorter survival.

In conclusion, this study demonstrates that tumour-infiltrating immune cells play a pivotal role in the tumour microenvironment and hold prognostic relevance in feline oral squamous cell carcinoma and osteosarcoma. Notably, higher infiltration of $CD3^+$ T cells, $CD8^+$ T cells and $CD20^+$ B cells was unexpectedly associated with shorter survival, suggesting that their accumulation may reflect immunosuppressive or dysfunctional responses rather than effective antitumour activity. These findings underscore the importance of further investigating immune regulatory pathways and checkpoint mechanisms in feline tumours to refine prognostic assessment and inform the development of targeted immunotherapeutic strategies.

TABLE OF CONTENT

SUMMARY ……..…….. i

TABLE OF CONTENT …….. iii

GENERAL INTRODUCTION ……... 1

Feline Malignancy ……. 1

Tumour-Infiltrating Immune Cells …… 2

Tumour-Infiltrating Immune Cells in Feline Oral Squamous Cell Carcinoma and Osteosarcoma ……... 5

CHAPTER I ……..... 8

1.1 Summary ……. 9

1.2 Introduction ……. 10

1.3 Materials and Methods …… 11

1.3.1 Samples …….. 11

1.3.2 Immunohistochemistry (IHC) ……..... 12

1.3.3 Evaluation and quantification of the immune cells ……... 12

1.3.4 Statistical analysis …….. 13

1.4 Result …….……. 13

1.4.1Immunohistochemical evaluation of tumour-infiltrating immune cells based on the areas ……... 13

1.4.2 Correlation between tumour-infiltrating immune cells and clinicopathological parameters in feline oral squamous cell carcinoma …...……. 14

1.4.3 Correlation between each type of tumour-infiltrating immune cells in feline oral squamous cell carcinoma 15
1.5 Discussion 16
1.6 Conclusions 19
1.7 Table Chapter I 21
1.8 Figure Chapter I 24
CHAPTER II 29
2.1 Summary 30
2.2 Introduction 31
2.3 Materials and Methods 32
2.3.1 Samples collection 32
2.3.2 Immunohistochemical labelling and evaluation 33
2.3.3 Tumour-infiltrating immune cells counting 35
2.3.4 Statistical analysis 36
2.4 Result 37
2.4.1 Demographic of feline osteosarcoma samples 37
2.4.2 Immunohistochemical evaluation of tumour-infiltrating immune cells in feline osteosarcoma 38
2.4.3 Correlation among tumour-infiltrating immune cell subsets 38
2.4.4 Correlation between clinical variables and tumour-infiltrating immune cells 38
2.5 Discussion 39
2.6 Conclusion 43

2.7 Table Chapter II ……... 44

2.8 Figure Chapter II ……. 46

GENERAL DISCUSSION ……... 48

ACKNOWLEDGMENT …… 51

REFERENCES ……... 53

APPENDICES …… 67

GENERAL INTRODUCTION

Feline Malignancy

Cancer is a major cause of morbidity and mortality in companion animals, including cats. A previous epidemiological study reported that cancer is the most common cause of death in cats, accounting for 1.113 cases (35.81%) (Kent *et al.,* 2022). Other studies have shown that feline tumours most often affect non-pedigree cats and exhibit malignant behaviour (Huber *et al*., 2024; Seung *et al.,* 2024). The most common cancers in cats include mammary gland tumours, skin tumours, and various sarcomas. In particular, squamous cell carcinoma is one of the most frequently diagnosed malignancies in cats (Huber *et al*., 2024; Joudžiukynienė, 2025; Laissaoui *et al*, 2024).

Feline oral squamous cell carcinoma is the most common malignant oral neoplasm in cats, accounting for approximately 60-70% of all oral tumours (Mikiewics *et al.*, 2019; Pérez-Enriquez *et al.*, 2020; Stebbins *et al*., 1989). It is an aggressive tumour that typically arises from the mucosal epithelium of the maxilla, sublingual or lingual, mandible and caudal pharyngeal (Soltero-Rivera *et al*., 2014; Strohmayer *et al*., 2020). Due to its aggressiveness and poor response to conventional treatment such as surgery,

feline oral squamous cell carcinoma carries a poor prognosis, with a reported median survival time of approximately 91 days (Soltero-Rivera *et al.*, 2014).

Feline osteosarcoma is the most common primary bone tumour in cats, accounting for approximately 70% of all primary bone tumours (Heldmann *et al.,* 2000; Liu *et al.,* 1974; Quiglay and Leedale, 1983). Unlike canine osteosarcoma, which is highly metastatic and aggressive, feline osteosarcoma typically exhibits slower progression and a lower rate of metastasis. In feline osteosarcoma, the appendicular skeleton is the most frequently affected site, followed by axial and extra-skeletal sites (Heldmann *et al.,* 2000; Nakano *et al.,* 2022). Within appendicular sites, the femur is the most involved, followed by the tibia-fibula, scapula, humerus, radius-ulna, digit of the hind limb and carpal region (Nakano *et al*., 2022). Cats with appendicular or extra-skeletal osteosarcoma generally have a longer survival than axial osteosarcoma (Heldmann *et al.,* 2000). In a recent retrospective study, the median survival time for appendicular feline osteosarcoma was reported to be approximately 527 days (Nakano *et al.,* 2022).

Tumour Infiltrating-Immune Cells

Whether innate or adaptive, tumour-infiltrating immune cells are a crucial component of the tumour microenvironment (TME), contributing to tumour progression and promising target for immunotherapy strategies (Gentles *et al*., 2015; Lv *et al*., 2022). These immune cells can be classified according to their functional roles within the TME into anti-tumour and promoting tumour growth. The former, including cytotoxic T lymphocytes (CTLs), natural killer (NK) cells, dendritic cells and M1-polarised macrophages, induce cytotoxic activity and mediate tumour cell elimination. In contrast, the latter, such as regulatory T cells (Tregs), myeloid-derived suppressor cells (MDSCs), M2-polarised macrophages, Type 2 Natural Killer T (NKT2) cells and Type 2 Innate Lymphoid cells (ILC2s), predominantly exert immunosuppressive effects that facilitate tumour proliferation, invasion and metastasis (Gajewski *et al*., 2013; Gentles *et al*., 2015; Lv *et al*., 2022).

The role and prognostic significance of tumour infiltrating-immune cells have been reported in various human cancer. In general, $CD3^+$ and $CD8^+$ cytotoxic T cell infiltration is associated with better clinical outcome in malignancies such as breast cancer, lung cancer and colorectal carcinoma (Barbosa *et al.*, 2021; Chen *et al.*, 2024;

Gooden *et al*., 2011; Kasurinen *et al.*, 2022; Li *et al*., 2022;). In contrast, an increased presence of immunosuppressive cell types, including $Foxp3^+$ Treg or M2-polarised macrophages, have been correlated with tumour aggressiveness, metastasis and shorter survival time (Chen *et al*., 2024; Miyasato *et al*., 2017; Shaopeng *et al*., 2024; Xie *et al.*, 2024). Interestingly, $CD20^+$ B cells have been reported to possess both anti-tumour and pro-tumourigenic activity, indicating a dual role in cancer immunity depending on the tumour type and microenvironmental context (Edin *et al.*, 2019; Sales de Sá *et al*., 2021; Suárez-Sánchez *et al*., 2021; Yuen *et el*., 2016). Collectively, these findings underscore the complexity of immune cells regulation within tumour microenvironment.

In veterinary oncology, studies of tumour infiltrating-immune cells have begun to elucidate the immunological mechanism underlying several animal tumours, including mammary tumour, oral squamous cell carcinoma and osteosarcoma (Boss *et al.*, 2023; Flecher *et al*., 2025; Sparger *et al.,* 2018; Withers *et al.*, 2019a). In both canine and feline tumour studies, $CD3^+$ and $CD8^+$ T lymphocytes infiltration have been associated with host immune activation, whereas the accumulation of M2-polarised macrophage ($CD204^+$) has been associated with increased malignancy and metastasis potential

(Nascimento *et al*., 2022; Pinard *et al*., 2022; Yokota *et al.,* 2023). These comparative insights emphasise the biological relevance of immune cells in naturally occurring animal tumour, providing valuable perspectives for both prognostic evaluation in veterinary oncology and advance comparative oncology research.

Tumour-Infiltrating Immune Cells in Feline Oral Squamous Cell Carcinoma and Osteosarcoma

From an immunological perspective, tumour-infiltrating immune cells play a significant role in tumourss progression and have been identified as potential target for immunotherapy (Hu *et al*., 2020; Liang *et al*., 2024). In human oncology, tumour-infiltrating lymphocytes have been correlated with improved outcomes in laryngeal squamous cell carcinoma (Zhang *et al*., 2021). Similarly, abundant $CD20^{+}$ B cell infiltration density has been correlated with better prognosis in human oral squamous cell carcinoma (Suárez-Sánchez *et al*., 2021). Conversely, increased tumour-associated macrophage (TAMs) infiltration, which promote immunosuppression and tumour cell development, has been associated with poor prognosis (Fujii *et al.,* 2012; Xue *et al*., 2022).

In feline oral squamous cell carcinoma, Sparger *et al.,* (2018) reported the presence of tumour-infiltrating lymphoid subset including T and B cells, within the tumour tissue.

In osteosarcoma, tumour-infiltrating immune cells have also been shown to influence disease progression and clinical outcome. In human osteosarcoma, high $CD8^+$ T cell infiltration has been associated with improved outcome and increased curability, particularly in axial osteosarcoma (Liu *et al.,* 2019). Similarly, study in other species have demonstrated that $CD3^+$ T cells infiltration associated with prolonged survival (Modiano *et al*., 2012). Conversely, Withers *et al*., (2019a) reported that in canine osteosarcoma, a higher $CD204^+$ macrophage infiltration, rather than $CD3^+$ T cells, was associated with better clinical outcomes, suggesting that immune regulation in TME may vary among species.

However, the correlation between these immune cells and clinicopathological condition or survival outcomes in feline tumour including oral squamous cell carcinoma or osteosarcoma have not been clearly elucidated. Understanding these interactions is expected to provide valuable insights into tumour biology and may contribute to the

identification of potential prognostic biomarkers and immunotherapeutic targets in feline malignancies.

Chapter 1

Investigation of Tumour-Infiltrating Immune Cells as a Prognostic Factor in Feline Oral Squamous Cell Carcinoma

1.1 Summary

This study aimed to evaluate the prognostic significance of tumour-infiltrating immune cells in feline oral squamous cell carcinoma (OSCC). Immunohistochemistry was used to quantify tumour-infiltrating immune cells in 20 feline OSCC samples. $CD3^+$ T, $CD8^+$ T, $Foxp3^+$ regulatory T and $CD20^+$ B cells and $CD204^+$ macrophages were assessed in both the tumour and stroma areas. Immune cell infiltration was more prominent in the stroma area, particularly for $CD20^+$ B cells. High $CD3^+$ T-cell and $CD20^+$ B-cell densities were negatively correlated with survival outcomes. Moreover, based on infiltration level, low densities of $CD3^+$ T cell infiltration were significantly associated with longer overall survival times. Likewise, low densities of $CD8^+$ T cells were linked with significantly longer progression-free intervals.

1.2 Introduction

Oral squamous cell carcinoma (OSCC), a malignant neoplasm, often occurs in cats (Cray *et al.,* 2020; Mikiewicz *et al.,* 2019). Feline OSCC originates from epithelial squamous cells and commonly occurs in the integument overlying the tongue, mandible, maxilla, caudal oral mucosa, vestibule and palatum durum (Soltero-Rivera *et al.*, 2014; Zaccone *et al*., 2021). Although metastasis is rare in cats, previous studies have reported that cats with OSCC present with metastasis to the mandibular lymph nodes and pulmonary area (Liptak *et al.,* 2021; Soltero-Rivera *et al.,* 2014). The survival rate of cats with OSCC is low, as reported previously (Soltero-Rivera *et al.*, 2014).

Tumour-infiltrating immune cells, including innate and adaptive immune cells, are critical components of the tumour microenvironment and crucial in tumour development. Several studies in humans have reported the relationship between tumour-infiltrating immune cells and the proliferation and progression of tumour cells, such as lung, cervical, nasopharyngeal, colorectal cancer and head and neck squamous cell carcinoma (Berntsson *et al.,* 2016; Caruntu *et al.,* 2021; Li *et al.,* 2022; Liu *et al.*, 2022, Liu *et al.*, 2017; Ye *et al.,* 2019; Zou *et al.*, 2021). Various densities of tumour-infiltrating immune cells have been associated with prognosis and survival in tumour cases. A study in humans revealed that high densities of tumour-infiltrating lymphocytes ($CD3^+$, $CD4^+$ and $CD8^+$) result in better overall survival and disease-free survival times in laryngeal squamous cell carcinoma (Zhang *et al.*, 2021). Similarly, $CD20^+$ B cells correlated with other infiltrating immune cells and better outcomes in OSCC (Suárez-Sánchez *et al.*, 2021). In contrast, tumour-associated macrophages stimulate proliferation, angiogenesis and immunosuppression, resulting in a worse prognosis in OSCC (Fujii *et al.*, 2012; Xue *et al.,* 2022; Yamagata *et al.,* 2017).

Recently, several studies have focused on the immune cells in feline tumours, such as in feline glioma, mammary carcinoma, melanocytic tumours and OSCC (Dagher *et al.*, 2020; Porcellato *et al.*, 2021; Rissi *et al.*, 2018; Sparger *et al.*, 2018). Unfortunately, Sparger *et al.,* (2018) did not investigate the correlation between immune cells and prognostic value. Therefore, the present study aimed to investigate tumour-infiltrating immune cells in the stroma and tumour areas and the relationship between tumour-infiltrating immune cells and clinicopathological parameters, as well as their potential prognostic value in cats with OSCC.

1.3 Materials and methods

1.3.1 Samples

This study used 20 surgically resected tumour tissue samples from cats diagnosed with feline OSCC whose clinical characteristics have been published already (Iwata *et al*., 2025). Samples were collected surgically from cats presented to the Japan Small Animal Cancer Center (Saitama, Japan) between January 2008 and December 2022. None of the cats received treatment, either chemotherapy or radiotherapy, providing a unique perspective on the natural course of the disease. The following clinical information, which was available from medical records (Table 1.1), was extracted from the published manuscript (Iwata *et al.,* 2025): sex, age, body weight, tumour size, tumour stage, lymph node metastasis, clinical stage appearance, recurrence, overall survival time (OST) and progression-free interval (PFI). The OST was defined as the period from tumour tissue resection to death or loss to follow-up, and the PFI was defined as the period from the tissue resection to the current state of the animal or the most recent information regarding progression up to the follow-up for our analysis.

1.3.2 Immunohistochemistry (IHC)

The formalin-fixed, paraffin-wax embedded tissue samples were sectioned (4 μm), de-paraffinised using xylene and rehydrated using graded alcohols. Subsequently, antigen retrieval was performed using citrate buffer solution or Dako Target Retrieval Solution, pH 9 (Agilent Technologies, www.agilent.com) in an autoclave (121°C, 20 min). Endogenous peroxidase activity was quenched with 3% H_2O_2 in methanol for 30 min, followed by blocking non-specific antibody binding with 5% skimmed milk and 5% bovine serum albumin in phosphate-buffered saline for 30 min at room temperature. Then, the slides were incubated with primary antibody, anti-CD3 mouse monoclonal antibody (clone F7.2.38, Santa Cruz Biotechnology, www.scbt.com), anti-CD8 rat monoclonal antibody (clone F3-B2, made in our laboratory) (Sakai *et al.,* 2020), anti-Foxp3 mouse monoclonal antibody (clone eBio7979, Life Technologies, www.thermofisher.com), anti-CD20 rabbit polyclonal antibody (ACROBiosystems, www.acrobiosystems.com), and macrophage marker anti-CD204 mouse monoclonal antibody (clone SRA-E5, Cosmobio, www.cosmobiousa.com). Subsequently, the slides were incubated with suitable secondary antibodies using Histofine Simple Stain Mouse MAX PO (Nichirei Bioscience Inc., https://nichireibiosiences. com), Histofine Simple Stain Rat MAX PO (Nichirei Bioscience Inc.), or Histofine Simple Stain Rabbit MAX PO (Nichirei Bioscience Inc.). The slides were visualised using a peroxidase staining diaminobenzidine kit (Nacalai Tesque, www.nacalai.com) and counterstained with Mayer's haematoxylin solution (FUJIFILM Wako Pure Chemical Corporation, www.fujifilm.com). Positive labelling was evaluated by comparison with haematoxylin and eosin (HE)-stained section.

1.3.3 Evaluation and quantification of the immune cells

The slides were scanned to enable manual assessment using ImageJ 1.53e. Immune cells were identified using specific markers (CD3, CD8, CD20, Foxp3 and CD204). Each sample was counted for 10 representative areas at ×200 magnification (0.204 mm^2). The total immune cell counts in the stroma and tumour areas were counted and averaged to determine the final density (cells/mm^2) (Fang *et al.*, 2017). The median value of each marker was also used as a cutoff value to differentiate between low and high infiltration.

1.3.4 Statistical analysis

Data were analysed using John's Macintosh Project (JMP) 18.0 (SAS Institute Japan, www.sas.com). Correlations among tumour-infiltrating immune cells densities were evaluated using Spearman's rank correlation test. Associations between clinical parameters and tumour-infiltrating immune cells densities were assessed using the Kruskal–Wallis test for categorical variables and Spearman's rank correlation test for continuous variables. The OST and PFI were evaluated using the Kaplan–Meier method. Differences between survival curves were analysed using the log-rank test for significance.

1.4 Results

1.4.1 Immunohistochemical evaluation of tumour-infiltrating immune cells based on the areas

Immunohistochemical evaluation of the immune cells is presented in Fig. 1.1a. Fig. 1.1b describe the frequency of each type of immune cell in feline OSCC based on the area. $CD3^+$ T cells were present in 95% (19/20) of feline OSCC cases, of which 18

were detected in either the stroma or tumour area. One case had $CD3^+$ T cells in the stroma area only. $CD8^+$ T cells were found in 80% (16/20) of the feline OSCC samples, eleven samples in the stroma and tumour areas, whereas in five samples only in the stroma. $Foxp3^+$ regulatory T cells (Tregs) were present in 25% (5/20) of cases of feline OSCC in the stroma or tumour areas. Ninety-five percent (19/20) of the cases had $CD20^+$ B cells present. Of these, nine had $CD20^+$ B cells in both the stroma and tumour areas, whereas 10 had them in the stroma only. Furthermore, all feline OSCC samples (20/20) had $CD204^+$ macrophages in the stroma and tumour areas with various densities.

Figure 1.1c and Supplementary Table 1 present the density of immune cells present in case of feline OSCC in the stroma and tumour areas. The average densities of $CD3^+$ T cells, $CD8^+$ T cells, $Foxp3^+$ Tregs, and $CD204^+$ macrophages in the stroma and tumour areas were 158.12 ± 231.44 (range, 0.00–838.36) cells/mm^2 and 88.27 ± 116.74 (range, 0.00–386.07) cells/mm^2, 56.35 ± 103.40 (range, 0.00–386.84) cells/mm^2 and 57.38 ± 123.29 (range, 0.00–375.12) cells/mm^2, 30.83 ± 74.43 (range, 0.00–306.29) cells/mm^2 and 6.48 ± 17.97 (range, 0.00–74.14) cells/mm^2 and 110.17 ± 124.69 (range, 10.9–409.8) cells/mm^2 and 71.58 ± 74.39 (range, 4.52–267.71) cells/mm^2, respectively, and those densities were not significantly different between the stroma and tumour areas. Conversely, the density of $CD20^+$ B cells was significantly higher in the stroma area than in the tumour area (67.79 ± 70.90 [range, 0.00–257.02] cell/mm^2 versus 6.64 ± 11.92 [range, 0.00–35.94] cell/mm^2, P <0.0001).

1.4.2 Correlation between each type of tumour-infiltrating immune cells in feline oral squamous cell carcinoma

In the stroma (Table 1.2), a high density of $CD3^+$ T cells correlated strongly with a high density of $CD8^+$ T cells (r = 0.8755, P <0.0001) and $CD20^+$ B cells (r = 0.7789, P <0.0001) and intermediately correlated with the density of $Foxp3^+$ Tregs (r = 0.6818, P = 0.0009). A strong and intermediate correlation was also observed between the increasing density of $CD8^+$ T cells with the density of $CD20^+$ B cells (r = 0.7193, P = 0.0004) and $Foxp3^+$ Tregs (r = 0.6844, P = 0.0009), respectively. Furthermore, a strong correlation was observed between stroma $Foxp3^+$ Tregs and stroma $CD204^+$ macrophages (r = 0.7253, P = 0.0003). An intermediate correlation was observed between stroma $CD3^+$ T cells and stroma $CD204^+$ macrophages (r = 0.4962, P = 0.0261) and stroma $CD8^+$ T cells and stroma $CD204^+$ macrophages (r = 0.4823, P = 0.0313).

In the tumour area (Table 1.3), intermediate correlations were found between $CD3^+$ T and $CD8^+$ T cells (r = 0.6624, P = 0.0015), $CD20^+$ B cells (r = 0.5352, P = 0.015) and $Foxp3^+$ Tregs (r = 0.6070, P = 0.0045). In addition, an intermediate correlation was observed between $CD8^+$ T cells and $CD20^+$ B cells (r = 0.5264, P = 0.0171) and $Foxp3^+$ Tregs (r = 0.6900, P = 0.0008). $CD204^+$ macrophages demonstrated an intermediate correlation with $CD3^+$ T cells (r = 0.5235, P = 0.0178), $CD8^+$ T cells (r = 0.6243, P = 0.0033), and $CD20^+$ B cells (r = 0.5564, P = 0.0108) and a strong correlation with $Foxp3^+$ Tregs (r = 0.7016, P = 0.0006).

1.4.3 Correlation between tumour-infiltrating immune cells and clinicopathological parameters in feline oral squamous cell carcinoma

Table 1.4 presents the correlation between the density of immune cell and clinicopathological parameters in feline OSCC. In our study, stroma $CD20^+$ B cells showed an intermediate negative correlation with the PFI (r = −0.4767, P = 0.0336).

Tumour $CD3^+$ T cells also showed an intermediate negative correlation with the PFI (r = −0.4551, $P = 0.0438$) and OST (r = −0.4866, $P = 0.0296$). The median immune cell count was used as a cutoff point for the difference between the high and low infiltration groups. Using the Kaplan–Meier method, high and low immune cell infiltration levels were compared with the PFI (Fig. 1.2) and OST (Fig. 1.3). The finding indicated that low stroma $CD8^+$ T cell infiltration had significantly longer PFI than high $CD8^+$ T cell infiltration ($P = 0.0346$). Moreover, low tumour $CD3^+$ T cell infiltration showed significantly longer OST than high infiltration ($P = 0.0092$). Although not statistically significant, cases with lower numbers of stroma $CD8^+$ T cells tended to have longer OSTs, consistent with the PFI results.

1.5 Discussion

This study found that the number of all immune cells in feline OSCC was higher in the stroma area. Furthermore, although only the density of $CD20^+$ B cells showed a significant difference between the stromal and intratumoural areas, the density of $CD3^+$ T cells, $Foxp3^+$ Tregs and $CD204^+$ macrophages tended to be higher in the stroma area than in the tumour area. As in the previous study on feline OSCC, immune cells were more numerous in the stroma area (Sparger *et al.,* 2018). Therefore, molecules such as proinflammatory cytokines (e.g., interleukin [IL]-6) and chemokines (e.g., chemokine (C-C motif) ligand 2 [CCL2]) in the stroma microenvironment may attract and modulate immune cells in OSCC (Rossi *et al.,* 2022).

In this study, a correlation was found between the immune cells in different areas. In the stroma, $CD3^+$ T cells strongly correlated with $CD8^+$ T and $CD20^+$ B cells while demonstrating a moderate correlation with $Foxp3^+$ Tregs and $CD204^+$ macrophages. In

the tumour area, $CD3^+$ T cells strongly correlated with $CD8^+$ T cells and moderately correlated with $CD20^+$ B cells, $Foxp3^+$ Tregs and $CD204^+$ macrophages. This finding is consistent with the results of previous studies on feline OSCC, which revealed that $CD3^+$ T cells correlated strongly with anti-CD79-labelled B cells and correlated moderately with $Foxp3^+$ Tregs (Sparger *et al.,* 2018). These findings indicate that immune cells respond to tumour cells in feline OSCC.

T or B immune cells have an antitumour function and are associated with better prognoses and outcomes in several tumour types, including OSCC (Berntsson *et al.*, 2016; Nascimento *et al*., 2022; Sales de Sá *et al.*, 2021; Suárez-Sánchez *et al.*, 2021; Wongpattaraworakul *et al*., 2024). However, contrary to previous studies, our results showed that higher infiltration of $CD3^+$ T cells, $CD8^+$ T cells and $CD20^+$ B cells was associated with poorer clinical outcomes in feline OSCC. Although no significant associations were observed between immune cells and clinicopathological features, we found a negative correlation between stroma $CD20^+$ B cells and the PFI. This finding differs from a previous report showing that $CD20^+$ B cells in human OSCC were positively correlated with survival, with median survival reaching 78.5 months (Sales de Sá *et al.*, 2021). This is intriguing, as $CD20^+$ B cells have been previously described as antitumourigenic in several cancers. However, recent studies suggest that B cells may also exhibit protumourigenic activity by secreting lymphotoxins that activate angiogenesis and oncogenic pathways such as NF-κB and STAT3 (Yuen *et al.,* 2016). Therefore, the role of $CD20^+$ B cells in feline OSCC may be context-dependent and warrants further functional investigation.

Similarly, a moderate negative correlation between tumour $CD3^+$ T cells infiltration and both OST and PFI was observed. Kaplan-Meier analysis further supported

this trend, with low infiltration of tumour $CD3^+$ and stroma $CD8^+$ T cells associated with better outcomes. These findings contrast with the general assumption that T cell infiltration confers improved prognosis. For example, in feline mammary carcinoma, $CD3^+$ T cells were the most prevalent immune cells subset and higher stroma $CD8^+$ T cell infiltration was correlated with longer survival and disease-free survival (Nascimento *et al*., 2022). One possible explanation is that the tumour microenvironment in feline OSCC may promote immune dysfunction despite high T cell presence (Caruntu *et al.,* 2021; Mukherjee *et al.,* 2020; Piersiala *et al.*, 2024; Rafiul *et al.,* 2019; Surendran *et al.*, 2022).

This hypothesis is supported by our observation that all cases expressed $CD204^+$ macrophages, which are thought to reflect the immune suppressive M2 phenotype in other species (Chaudari *et al.,* 2021). Although we could not distinguish M1 from M2 macrophages in this study, previous research has shown that M2 macrophage can inhibit $CD8^+$ T-cell function by releasing immunosuppressive factors such as CCL2, IL-10, TGF-β and PD-L1 (Kahdeh *et al*., 2024; Kondo *et al*., 2021; Kubota *et al.*, 2017; Tang *et al*., 2017; Xue *et al.*, 2022). Furthermore, the presence of $Foxp3^+$ Tregs in some cases may have also contributed to the immunosuppressive tumour milieu. While no significant association with survival was found, Tregs are known to secrete cytokines, such as TGF-β, IL-35 and IL-10, which suppress $CD8^+$ cytotoxic T cells (Perri *et al.*, 2020). A previous study by Sparger *et al.,* (2018) also suggested that COX2 expression may contribute to $CD8^+$ T-cell dysfunction, although no direct analysis was performed.

Another plausible mechanism is T-cell exhaustion, a phenomenon where chronic antigen stimulation leads to T cells losing their effector functions and upregulating inhibitory receptors such as cytotoxic T-lymphocyte-associated protein 4, programmed death-1, T-cell immunoglobulin and mucin domain-containing protein-3 and lymphocyte

activation gene 3 (Binnewies *et al.,* 2018; Pauken and Wherry, 2015). Although T-cell exhaustion is a reasonable hypothesis to explain our findings, this study did not assess the expression of exhaustion markers or functional cytokine production, and thus this interpretation remains speculative. Further research using molecular markers or functional assays will be required to investigate this possibility. In addition, although $CD204^+$ macrophages and $Foxp3^+$ Tregs were detected and showed significant correlations with other immune cell types, neither was directly associated with survival in our cohort. Therefore, their role in modulating the immune landscape and indirectly shaping clinical outcomes should be explored in future studies.

Taken together, the presence of high densities of T and B cells in feline OSCC does not necessarily indicate effective antitumour immunity. In contrast to previous human OSCC studies reporting that elevated T and B cell infiltration is associated with improved outcomes (Sales de Sá *et al.*, 2021; Suárez-Sánchez *et al.*, 2021; Wongpattaraworakul *et al*., 2024), our findings suggest that in feline OSCC these immune cells may be functionally impaired or reprogrammed within a suppressive microenvironment.

1.6 Conclusions

Tumour-infiltrating immune cells play a crucial role in the tumour microenvironment and have potential prognostic significance in feline OSCC. In this study, infiltration by greater number of $CD3^+$ T cells, $CD8^+$ T cells, and $CD20^+$ B cells was unexpectedly associated with shorter survival outcomes. These findings underscore the complexity of immune cell interactions within the tumour microenvironment in feline OSCC. Further studies are warranted to clarify the functional roles of these immune cells

and their regulatory mechanisms, including immune checkpoint pathways and T-cell exhaustion, to better understand their impact on prognosis and therapeutic response.

1.7 Tables of Chapter I

Table 1.1 Clinicopathological parameters of feline oral squamous cell carcinoma cases.

Clinicopathological Parameters	
Age, (mean ± SD, year)	11.85 ± 2.35
Body weight, (mean ± SD, kg)	3.95 ± 0.97
Tumour size, (mean ± SD, mm)	36.28 ± 9.49
Tumour stage, n (%)	
Stage 1	1 (5)
Stage 2	14 (70)
Stage 3	5 (25)
Lymph node metastasis, n (%)	
Absent	18 (90)
Present	2 (10)
Clinical stage appearance, n (%)	
Mild	1 (5)
Moderate	13 (65)
Severe	6 (30)
Tumour recurrence, n (%)	
Absent	14 (70)
Present	6 (30)
Overall survival time, median (, days)	533 (182–1,665)
Progression-free interval, median (range, days)	914 (174–not to reached)

Table 1.2 Spearman's correlation between tumour-infiltrating immune cell densities in the stroma area.

Immune cells	$CD3^+$ T cells	$CD8^+$ T cells	$CD20^+$ B cells	$Foxp3^+$ Tregs	$CD204^+$ macrophages
$CD3^+$ T cells	1	0.8755	0.7789	0.6818	0.4962
	1	< 0.0001*	< 0.0001*	0.0009*	0.0261*
$CD8^+$ T cells		1	0.7193	0.6844	0.4823
		1	0.0004*	0.0009*	0.0313*
$CD20^+$ B cells			1	0.3854	0.2827
			1	0.0933	0.2272
$Foxp3^+$ Tregs				1	0.7253
				1	0.0003*
$CD204^+$ macrophages					1
					1

The first and second rows show the Spearman's correlation *r* value for each variable and the *P* value, respectively. * *P* <0,05.

Table 1.3 Spearman's correlation between tumour-infiltrating immune cell densities in the tumour area.

	$CD3^+$ T cells	$CD8^+$ T cells	$CD20^+$ B cells	$Foxp3^+$ Tregs	$CD204^+$ macrophages
$CD3^+$ T cells	1	0.6624	0.5352	0.607	0.5235
	1	0.0015*	0.015*	0.0045*	0.0178*
$CD8^+$ T cells		1	0.5264	0.69	0.6243
		1	0.0171*	0.0008*	0.0033*
$CD20^+$ B cells			1	0.3916	0.5564
			1	0.0878	0.0108*
$Foxp3^+$ Tregs				1	0.7016
				1	0.0006*
$CD204^+$ macrophages					1
					1

The first and second rows show the Spearman's correlation *r* value for each variable and the *P* value, respectively. * *P* <0,05.

Table 1.4 Correlation between the tumour-infiltrating immune cell density with clinicopathological parameters in feline oral squamous cell carcinoma.

Clinicopathological parameters	$CD3^+$ T cells		$CD8^+$ T cells		$CD20^+$ B cells		$Foxp3^+$ Tregs		$CD204^+$ macrophages	
	Stroma	**Tumour**	**Stroma**	**Tumour**	**Stroma**	**Tumour**	**Stroma**	**Tumour**	**Stroma**	**Tumour**
Sex[a]	−0.1019	−0.1869	−0.1961	−0.1781	0.1359	0.1674	−0.2233	−0.2456	−0.2039	0.1359
	0.6485	0.4031	0.3805	0.4257	0.5433	0.4542	0.3180	0.2721	0.3619	0.5433
Age[b]	−0.1165	−0.1387	−0.0845	−0.1070	−0.1379	−0.266	−0.0811	−0.0851	−0.0868	−0.307
	0.6246	0.5598	0.7232	0.6534	0.5622	0.2570	0.7340	0.7213	0.7159	0.1880
Body weight[b]	0.0987	0.0580	−0.0352	−0.1066	0.1702	0.1682	−0.2406	−0.2247	−0.3345	−0.0407
	0.6789	0.8080	0.8830	0.6546	0.4730	0.4784	0.3070	0.3408	0.1495	0.8648
Tumour size[b]	−0.0752	0.1030	−0.0664	0.0662	0.1414	0.2337	−0.2154	−0.2431	−0.0632	−0.0932
	0.7527	0.6655	0.7809	0.7815	0.5522	0.3213	0.3617	0.3017	0.7914	0.6958
Tumour stage[a]	−0.1833	−0.1163	−0.2058	−0.1515	−0.0402	−0.1864	−0.2151	−0.2125	−0.2127	−0.1706
	0.6427	0.3636	0.7783	0.4907	0.1905	0.6597	0.8426	0.8240	0.8253	0.5771
Lymph node metastasis[a]	0.1549	0.1268	−0.0424	0.1329	0.0704	0.3855	−0.1666	−0.1666	0.0704	0.2395
	0.4884	0.5706	0.8495	0.5522	0.7528	0.0847	0.4562	0.4562	0.7055	0.2842
Clinical stage appearance[a]	−0.1743	−0.1177	−0.2087	−0.1588	−0.1021	−0.1711	−0.2060	−0.2000	−0.2097	−0.1787
	0.5956	0.3680	0.7977	0.5220	0.3224	0.5796	0.7799	0.7407	0.8043	0.6182
Recurrence[a]	0.0092	0.3229	0.1388	−0.0483	0.0646	0.0000	0.1333	0.1333	0.0277	0.0646
	0.9343	0.1488	0.5346	0.8288	0.7728	1.0000	0.5510	0.5154	0.9015	0.7728
Overall survival time[b]	−0.4000	−0.4866	−0.3117	−0.3421	−0.4346	−0.1613	−0.1028	−0.0850	0.0301	−0.2767
	0.0806	0.0296*	0.1810	0.1398	0.0555	0.4969	0.6664	0.7217	0.8998	0.2376
Progression-free survival[b]	−0.3910	−0.4551	−0.3389	−0.3500	−0.4767	−0.1959	−0.0791	−0.0573	0.0241	−0.2526
	0.0883	0.0438*	0.1439	0.1303	0.0336*	0.4079	0.7404	0.8103	0.9198	0.2826

The first and second rows show the effect size (r or η^2 value) for each variable and the *P* value, respectively. * $P < 0.05$. [a] Data were analysed using Kruskal–Wallis test; [b] Data were analysed using Spearman's correlation test.

1.8 Figures of Chapter I

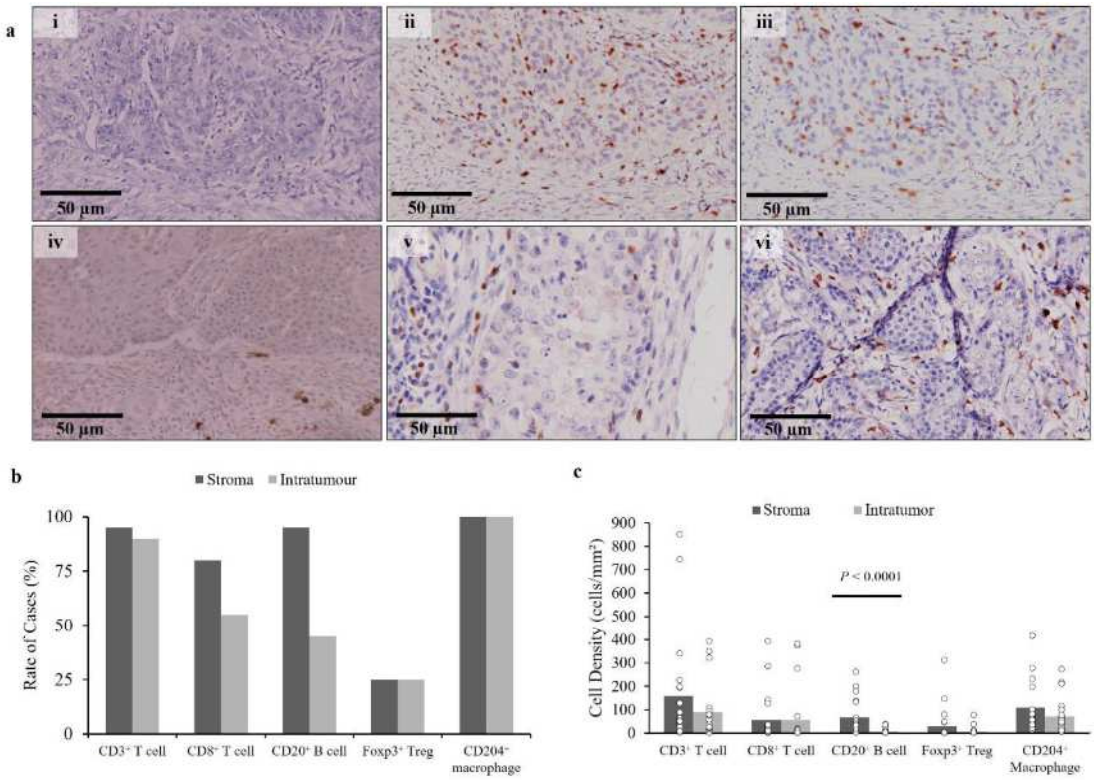


Figure 1.1 Tumour-infiltrating immune cells, feline oral squamous cell carcinoma (OSCC). (a) HE-stain and immunohistochemistry, ×400: (i) HE stain, (ii) $CD3^+$ T cells, (iii) $CD8^+$ T cells, (iv) $CD20^+$ B cells, (v) $Foxp3^+$ Tregs, and (vi) $CD204^+$ macrophages. (b) Comparison of percentage of cases in each tumour-infiltrating immune cell in feline OSCC based on area. (c) Comparison of density of each type of tumour-infiltrating immune cell in stroma and tumour areas of feline OSCC. Each dot represents the density of immune cells in an individual case, and the bars represent the mean of the group.

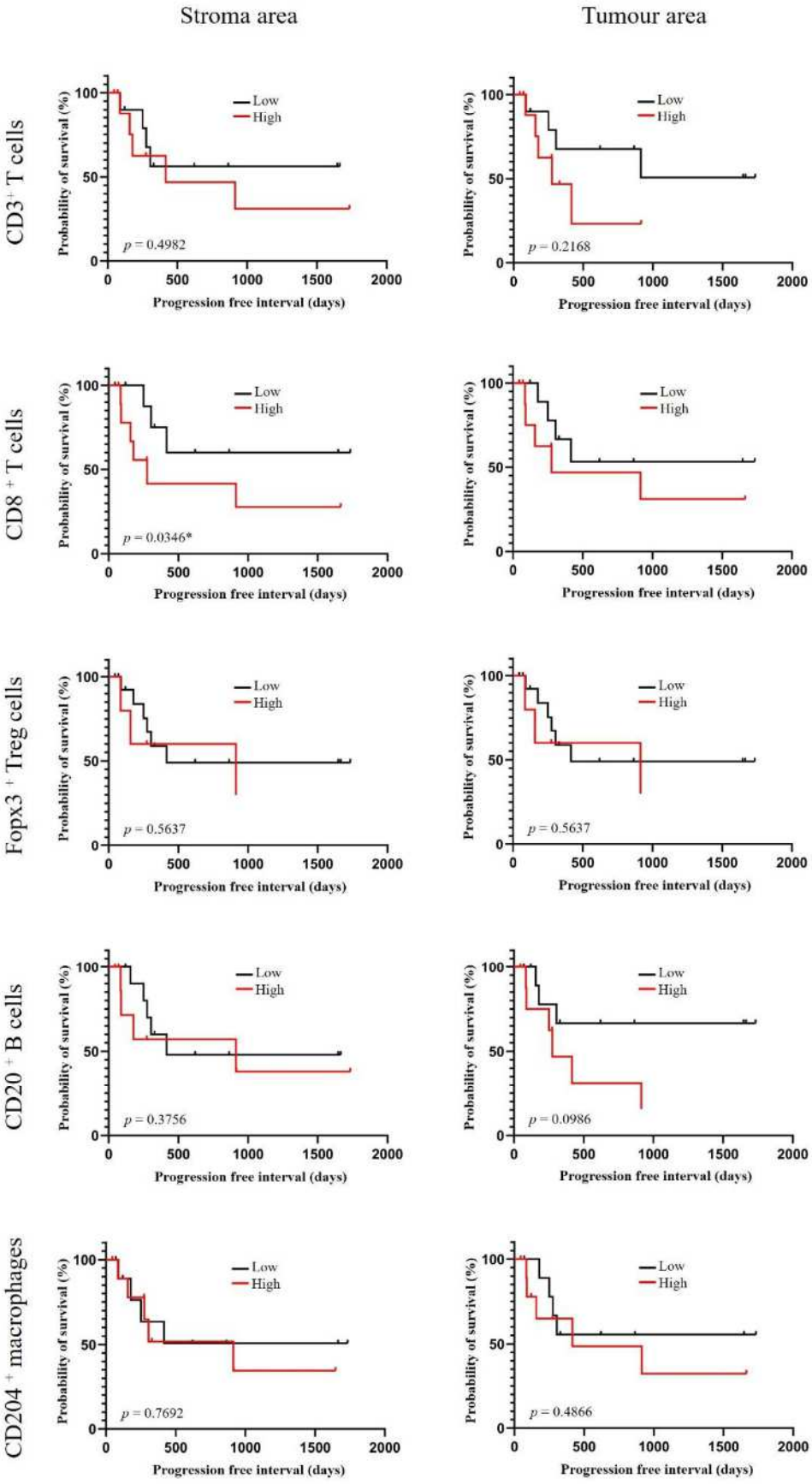

Stroma area
Tumour area
CD3+ T cells
CD8+ T cells
Foxp3+ Treg cells
CD20+ B cells
CD204+ macrophages
Probability of survival (%)
Progression free interval (days)
Low
High
p = 0.4982
p = 0.2168
p = 0.0346*
p = 0.5637
p = 0.5637
p = 0.3756
p = 0.0986
p = 0.7692
p = 0.4866

Figure 1. 2 Progression-free interval for the high and low groups of each type of immune cell in the stroma and tumour areas of feline oral squamous cell carcinoma. *P* value was estimated with the Kaplan–Meier log-rank test. Tick marks ("|") indicate censored observations.

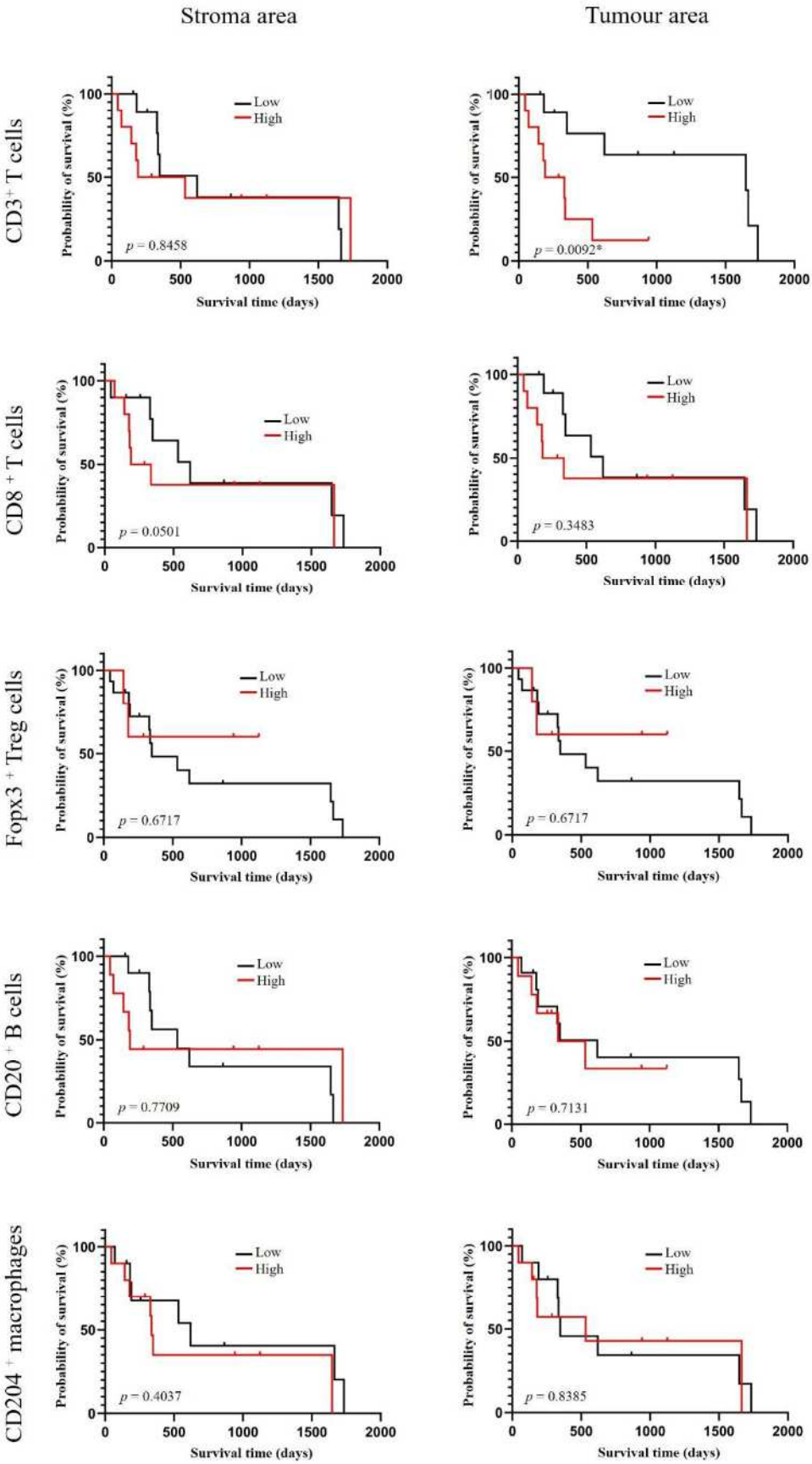

Stroma area
Tumour area
CD3+ T cells
CD8 + T cells
Fopx3 + Treg cells
CD20 + B cells
CD204 + macrophages
Probability of survival (%)
Survival time (days)
Low
High
p = 0.8458
p = 0.0092*
p = 0.0501
p = 0.3483
p = 0.6717
p = 0.6717
p = 0.7709
p = 0.7131
p = 0.4037
p = 0.8385

Figure 1.3 Overall survival time for the high and low groups of each type of immune cells in the stroma and tumour areas of feline oral squamous cell carcinoma. *P* value was estimated with Kaplan–Meier log-rank test. Tick marks ("|") indicate censored observations.

Chapter II

Evaluation of Tumour-Infiltrating Immune Cells and Their Prognostic Value in Feline Appendicular Osteosarcoma: A Pilot Study

2.1 Summary

This study aimed to evaluate the prognostic relevance of selected immune cell markers in feline appendicular osteosarcoma in relation to clinical outcome. We retrospectively profiled tumour-infiltrating immune cells in 16 primary tumours by immunohistochemistry for CD3, CD8, Foxp3, CD20 and CD204. Immune cell densities were quantified and correlated with clinicopathological features, and the Kaplan–Meier estimator assessed survival. $CD204^+$ macrophages were the most abundant population. Kaplan–Meier analysis revealed that higher intratumoural $CD3^+$ T and CD8+T cell densities were associated with shorter survival, and $CD3^+$, $CD8^+$ and $CD204^+$ densities showed strong positive co-infiltration, consistent with an inflamed yet potentially functionally constrained tumour microenvironment. $Foxp3^+$ cells were rarely detected, and age correlated inversely with $CD3^+$ and $CD8^+$ density. These observations suggest that T-cell quantity may not equate to anti-tumour quality in macrophage-rich feline osteosarcoma. However, the small retrospective cohort, univariable analyses without multiplicity adjustment and the absence of spatial or functional markers limit inference. These findings should be considered a hypothesis-generating, prospective validation integrating spatial profiling and checkpoint/exhaustion markers, and refined macrophage phenotyping is warranted before prognostic application.

2.2 Introduction

Osteosarcoma is the most prevalent primary bone tumour in cats (Liu *et al*., 1974; Quigley and Leedale, 1983). The characteristics of feline osteosarcoma are distinct from those of humans and dogs in that feline osteosarcoma has a lower metastatic rate and reduced aggressiveness (Bjørland *et al.,* 2005; Marconato *et al.,* 2024) and cats with osteosarcoma tend to have a longer survival time than dogs (Boston *et al.,* 2006; Marconato *et al.,* 2024; Nakano *et al.,* 2022; Withers *et al.,* 2019b). Despite these differences, the tumour microenvironment and immune components of feline osteosarcoma remain inadequately understood.

Tumour-infiltrating immune cells are a significant component of the tumour microenvironment (TME) and play a critical role in tumour progression, serving as potential therapeutic targets (Gentles *et al.,* 2015). Immune cells within the TME can be classified into anti-tumour immune cells that mediate tumour cell elimination and tumour-promoting immune cells that contribute to an immunosuppressive environment. Anti-tumour immune cells include natural killer cells, dendritic cells, $CD8^+$ cytotoxic T cells, $CD4^+$ effector T cells, N1-polarised neutrophils and M1-polarised macrophages. In contrast, tumour-promoting immune cells comprise myeloid-derived suppressor cells, regulatory T cells (Tregs), N2-polarised neutrophils and M2-polarszed macrophages (Gentles *et al.,* 2015; Giraldo *et al.*, 2019; Lv *et al.,* 2022).

In studies of human osteosarcoma, a high density of $CD8^+$ cytotoxic T cells has been associated with improved patient survival and suppression of metastasis (Casanova *et al*., 2021; Fritzsching *et al*., 2015; Liu *et al*., 2019). Conversely, an increased density of $Foxp3^+$ regulatory T cell is correlated with a poor prognosis (Fritzsching *et al*., 2015). Another study has indicated that patients with non-metastatic osteosarcoma contain high

numbers of NK cells, immature B cells, M1 macrophages, and neutrophils, along with lower numbers of M2 macrophages (Yang *et al.*, 2021). Thus, tumour-infiltrating immune cells are integral to osteosarcoma progression in humans.

In canine osteosarcoma, studies have shown that elevated levels of $CD3^+$ T cells correlate with improved survival following gene therapy (Modiano *et al*., 2012). In contrast, Withers *et al.,* (2019a) reported that $CD3^+$ infiltration was not significantly associated with survival, whereas tumours with higher densities of $CD204^+$ macrophages were associated with a longer disease-free interval. Furthermore, another canine and human osteosarcoma study reported elevated levels of T cells, B cells and macrophages in cases of pulmonary metastasis (Ligon *et al.*, 2021; Withers *et al*., 2019b). Although feline and canine osteosarcomas have been reported to have comparable histological features, their clinical outcomes differ substantially (Dimopoulou *et al.,* 2008). Moreover, the biological factors underlying this discrepancy remain poorly elucidated, and information regarding the characteristics and mechanisms of tumour-infiltrating immune cells in feline osteosarcoma is limited, particularly in relation to prognosis. Accordingly, the objective of the study was to characterise the tumour-infiltrating immune cells in feline osteosarcoma, thereby enhancing our understanding of its pathogenesis and identifying potential prognostic markers.

2.3 Materials and methods

2.3.1 Samples collection

Sixteen feline tumour tissue samples were collected from cats with appendicular osteosarcoma that underwent limb amputation as an aggressive focal treatment approach. These samples constituted a subset of cases from the cohort previously reported by

Nakano *et al.,* (2022) that were obtained exclusively at the Japan Small Animal Cancer Center (Saitama, Japan) between April 2007 and November 2012. For each case, clinical information was recorded, including sex, age, bodyweight, tumour location, radiographic abnormalities, lameness, metastasis at diagnosis, lymph node metastasis, distant metastasis, local recurrence, clinical outcome and overall survival time (OST). Clinical outcome was defined as survival status (dead, alive or unknown) at follow-up after amputation. OST was defined as the duration from surgical tumour resection to death from any cause or the date of last follow-up, with cats alive at last contact right-censored at the date.

2.3.2 Immunohistochemical labelling and evaluation

Tissue specimens preserved in 10% neutral pH phosphate-buffered formalin overnight were decalcified for 24 h using Decalx (Jokoh, https://jokoh.com), processed routinely through graded alcohols, embedded in paraffin wax and sectioned (4 μm). During the initial diagnostic process, multiple tissue sections were sampled from various regions of each tumour to ensure an accurate pathological diagnosis. For the immunohistochemical analysis, one representative formalin-fixed paraffin wax-embedded block per case was utilised. To ensure representativeness and minimise sampling bias, a veterinary pathologist reviewed all available initial haematoxylin and eosin (HE)-stained tissue section from each case and selected the most appropriate block containing the largest area of viable tumour tissue, carefully excluding areas of extensive necrosis and predominantly osteoid matrix. The tissue sections were deparaffinised with xylene and rehydrated through graded alcohols. Antigen retrieval was performed using a citrate buffer solution (pH 6.0) for antibodies against CD3, CD8, CD20 and CD204,

whereas Foxp3 labelling was performed using Dako Target Retrieval Solution pH 9.0 (Agilent Technologies, www.agilent.com) in an autoclave at 121°C for 20 min. To inhibit endogenous peroxidase activity, the slides were treated with 3% hydrogen peroxide in methanol for 30 min. Blocking of non-specific antibody binding was by a mixture of 5% skimmed milk and 5% bovine serum albumin in phosphate-buffered saline at room temperature for 30 min.

Subsequently, the sections were incubated with primary antibodies, including anti-CD3 mouse monoclonal antibody, dilution 1:20 (clone F7.2.38; Santa Cruz Biotechnology, www.scbt.com), anti-CD8 rat monoclonal antibody, dilution 5 µg/ml (clone F3-B2; produced in our laboratory) (Sakai *et al*., 2020), anti-Foxp3 mouse monoclonal antibody, dilution 1:100 (clone eBio7979; Life Technologies, www.thermofisher.com), anti-CD20 rabbit polyclonal antibody, dilution 1:100 (ACROBiosystems, www.acrobiosystems.com) and anti-CD204 mouse monoclonal antibody, dilution 1:400 (clone SRA-E5; Cosmo Bio, www.cosmobiousa.com), a marker for macrophages. Following primary antibody labelling, appropriate secondary antibodies were applied using Histofine Simple Stain systems: Mouse MAX PO, Rat MAX PO or Rabbit MAX PO (Nichirei Biosciences Inc., https://nichireibiosciences.com). Visualisation was performed using a peroxidase-based diaminobenzidine (DAB) staining kit (Nacalai Tesque, www.nacalai.com) and the slides were counterstained with Mayer's haematoxylin (FUJIFILM Wako Pure Chemical Corporation, www.fujifilm.com). To ensure the reliability of the immunohistochemistry (IHC) markers on decalcified tissues, normal lymphocytes and macrophages infiltrating the tissues were evaluated as internal positive controls to confirm the preservation of antigenicity. Specificity was verified by the absence of non-specific background labelling in the osteoid matrix or necrotic areas.

Furthermore, negative control slides, in which the primary antibody was replaced with an isotype-matched control antibody, were included in every batch of sections to confirm the absence of non-specific and off-target binding.

2.3.3 Tumour-infiltrating immune cells counting

The slides were scanned using a NanoZoomer-SQ scanner (Hamamatsu, www.hamamatsu.com) at ×10 magnification and visualised using NDP.view software (version 2.9.29). To quantify the immune cells, 10 individual non-consecutive fields were randomly selected within the tumour core at ×400 magnification and measured using ImageJ 1.53e software (NIH, www.imagej.net/ij/). The tumour core was morphologically defined as the central region of the tumour mass, avoiding the infiltrating margins. The selected area strictly represented viable tumour tissue, excluding massive necrotic areas, extensive osteoid matrix (as the inclusion of acellular matrix would artificially dilute the immune cell density calculation) and tissue artifacts. These 10 fields were chosen afresh for each marker. Each of the 10 fields had an identical area of 0.165 mm^2 (3,429,120 pixels) resulting in a total evaluated area of 1.65 mm^2 (10 × 0.165 mm^2) per cell marker for each area. Immune cells expressing CD3, CD8, Foxp3, CD20 and CD204 were counted manually. To minimise observational bias, all cell counts were performed by a single investigator who was blinded to the clinical outcomes and clinicopathological data of the cats. The counts were then converted to immune cell density (cells/mm^2) as described in our recently published study (Mihardi *et al*., 2025). During the quantification of $CD204^+$ cells, morphologically distinct osteoclasts (ie, multinucleated giant cells associated with bone matrix) were excluded from the counts to ensure only mononuclear tumour-infiltrating macrophages were evaluated. For each case, the mean density

calculated from these 10 fields was used as the representative global immune cell density for the entire tumour core (Fang *et al*., 2017). The median value of each marker was used as a cut-off value to differentiate between low and high infiltration. The calculations were performed using the following formulae:

$$\text{Tumour area (mm}^2\text{)} = \frac{\text{Tumour area (pixels)}}{3{,}429{,}120 \text{ pixels}} \text{ x } 0.165 \text{ mm}^2$$

$$\text{Immune cell density (cell/mm}^2\text{)} = \frac{\text{Number of immune cells}}{\text{Tumour area (mm}^2\text{)}}$$

2.3.4 Statistical analysis

Statistical analyses were conducted using John's Macintosh Project (JMP) version 18.0.2 (SAS Institute Japan, www.sas.com). Associations between clinical parameters and tumour-infiltrating immune cells were assessed with the Kruskal–Wallis test or Spearman's correlation test, as appropriate. Correlations among tumour-infiltrating immune cell densities were examined using Spearman's correlation test. For survival analysis, the cohort was divided into two groups based on the immune cell density. Because the immune cell densities across the cohort did not strictly follow a normal distribution, the median density of the entire cohort was utilised as a robust cut-off value. Cases with a representative mean density higher than the cohort median were classified as the 'high infiltration' group, whereas those with a density equal to or lower than the median were classified as the 'low infiltration' group.

2.4 Results

2.4.1 Demographics of feline osteosarcoma samples

The baseline clinical features of the feline osteosarcoma cases are shown in Table 2.1. Sixteen samples were obtained from cats diagnosed with osteosarcoma, with a mean ± SD age of 9.44 ± 5.02 years and a mean ± SD bodyweight of 4.25 ± 1.79 kg. Primary sites included the femur (6/16), humerus (3/16), radius (2/16), tibia (2/16), distal radius/ulna region (2/16) and scapula (1/16). None of the tumours involved extension across joint spaces. Radiographic abnormalities and lameness were documented in 15/16 cases (93.8%). At the time of initial diagnosis, only 1/16 (6.3%) cats presented with metastasis, which was specifically a distant metastasis. Over the entire clinical course, regional lymph node metastasis was identified in 1/16 (6.3%) cats at 93 days after amputation. Distant metastases were present in a total of 7/16 (43.8%) cats (including the one present at diagnosis) at various time points after surgery, with lung metastasis as the predominant site (five of seven cases), followed by the skin and subcutaneous tissue, the parasternal and left ilium regions and the collateral stifle region. Local recurrence was observed in one cat (6.3%) 267 days after limb amputation, with a survival time of 489 days after surgery; local recurrence was absent in 13/16 cats (81.3%) and unknown in 2/16 cats (12.5%). Regarding the final clinical outcomes at the end of the follow-up period, 10/16 cats (62.5%) had died with five tumour-related, two non-tumour-related deaths and three of unknown cause; 4/16 cats (25.0%) were alive and 2/16 cats (12.5%) had an unknown status. Notably, six of seven cats that developed distant metastasis were included in the group of cats that had died. Due to the study's retrospective design, complete follow-up was not available for all cases. The median OST was 320 days; range 156.5–608.25 days.

2.4.2 Immunohistochemical evaluation of tumour-infiltrating immune cells in feline osteosarcoma

Immunolabeling for CD3 (T cells), CD8 (cytotoxic T cells), Foxp3 (Treg cells) and CD20 (B cells) was detected in 15/16 (93.8%), 14/16 (87.5%), 2/16 (12.5%) and 10/16 (62.5%) tumours, respectively (Figure 1a). All tumours (16/16) contained $CD204^+$ macrophages at variable densities. Quantitative cell densities are summarised in Figure 2.1b and Supplementary Table 2. $CD204^+$ macrophages were the most abundant population (median and interquatile range [IQR], 681.34 [459.87 – 1,000.33] cells/mm^2). Median densities and IQR (cells/mm^2) of other subsets were: $CD3^+$ T cells, 89.08 [45.37 – 306.37]; $CD8^+$ T cells, 66.93 [24.20 – 235.74]; $Foxp3^+$ Treg cells, 0.00 [0.00 – 0.00]; and $CD20^+$ B cells, 28.86 [0.00 – 50.64].

2.4.3 Correlation among tumour-infiltrating immune cell subsets

Results of the Spearman's correlation test are summarised in Table 2.2. Pairwise correlations revealed a strong association between $CD3^+$ and $CD8^+$ T cells densities ($r = 0.9389$, $P < 0.0001$) and between $CD3^+$ T cells and $CD204^+$ macrophages ($r = 0.7147$, $P = 0.0019$). A moderate correlation was also observed between $CD8^+$ T cells with $CD204^+$ macrophages ($r = 0.6814$, $P = 0.0037$).

2.4.4 Correlation between clinical features and tumour-infiltrating immune cells

As shown in Supplementary Table 3, higher $CD3^+$ T cell density was significantly associated with clinical outcome (vital status) ($P = 0.0137$, $\eta^2 = 0.5057$), with weaker associations observed for $CD8^+$ T cells ($P = 0.0389$, $\eta^2 = 0.1454$) and $CD204^+$ macrophages ($P = 0.0464$, $\eta^2 = 0.2465$). Additionally, $CD3^+$ and $CD8^+$ T cell densities

were moderately negatively correlated with age (r = -0.5856, *P* = 0.0278; r = -0.5918, *P* = 0.0258), suggesting an age-related decline in immune surveillance. Crucially, time-to-event analysis using, the Kaplan–Meier estimator revealed that cases with higher $CD3^+$ and $CD8^+$ T cell densities had shorter OSTs (*P* = 0.0037; Figure 2.2).

2.5 Discussion

In this study of feline osteosarcoma, we found that higher intratumoural densities of $CD3^+$ T cells and $CD8^+$ T cells were associated with shorter OST. Although $CD204^+$ macrophages were the most abundant immune population across tumours, their density was not directly associated with survival. However, the strong positive correlations observed between $CD3^+$, $CD8^+$ and $CD204^+$ cells indicate that tumours with higher T-cell infiltration also have increased densities of macrophage infiltration, suggesting an inflamed yet potentially dysfunctional TME (Casanova *et al.,* 2021; Koirala *et al.*, 2016; Ligon *et al*., 2021).

Macrophage predominance is consistent with previous findings in canine and human osteosarcomas (Ligon *et al.,* 2021; Mannheimer *et al.,* 2023). However, while CD204 is widely recognized as a marker for M2-polarized tumour-associated macrophages in other species, comprehensive validation of its specific polarization status in feline tissues remains limited. Therefore, it is often utilized as a broader marker for tumour-infiltrating macrophages in cats (Mandara *et al.,* 2025; Mihardi *et al*., 2025). Thus, the present findings indicate macrophage abundance rather than mechanistically proving M2 dominance.

In our study, higher densities of $CD3^+$ T and $CD8^+$ T cells were associated with shorter OST, which is consistent with our previous study of feline oral squamous cell

carcinoma that showed that high densities of $CD3^+$ T and $CD8^+$ T cells were associated with a poorer outcome (Mihardi *et al.,* 2025). This finding, which contrasts with reports from several human and some canine studies, can be interpreted in several non-exclusive ways. First, T-cell infiltration may reflect a bystander or exhaustion response rather than effective cytotoxic immunity (Cheng *et al.,* 2024; Razmara *et al.,* 2021; Sun *et al.*, 2021). Second, macrophage-rich milieus can co-exist with T-cell influx yet limit function through tumour-associated macrophages, including $CD204^+$ macrophages, which release checkpoint ligands and immunoregulatory cytokines (Koirala *et al.*, 2016; Luo *et al.,* 2020; Ruffell *et al.,* 2014; Tatsuno *et al.,* 2024). Third, as detailed in the Materials and methods section, our quantification relied entirely on randomly selected fields within the tumour core. This approach inherently does not capture the macro-spatial architecture of the immune infiltrate, such as evaluating the infiltrating margins for 'immune-excluded' versus diffusely 'infiltrated' patterns. The lack of this broader spatial context could reconcile why dense local counts in the core did not relate to effective tumour control (Tsujikawa *et al.*, 2020; Zhou *et al.,* 2024). These interpretations are consistent with the strong positive correlations among T cells and $CD204^+$ macrophages, pointing to 'inflamed but suppressed' TMEs rather than purely 'cold' tumours, which is typically defined as low immune cell infiltration (Ding *et al*., 2025; Tatsuno *et al*., 2024; Xie *et al*., 2024).

Mechanistically, it is plausible that macrophage-mediated regulation (eg, PD-1/PD-L1 axes, IL-10/TGF-β signalling) contributes to T-cell dysfunction (Abd Elmoneim *et al.*, 2023; Cheng *et al.,* 2024; Guangning *et al.,* 2023; Hashimoto *et al.,* 2020; Koirala *et al.,* 2016; Luo *et al.,* 2020; Ruffell *et al.*, 2014; Sun et al., 2021; Tauriello *et al.*, 2018; Xia *et al.,* 2021;); however, our study did not directly measure checkpoint expression,

ligand co-localization or T-cell functional states. Therefore, we frame these as hypotheses rather than conclusions. Future work should incorporate multi-marker panels (eg, PD-1, PD-L1, LAG-3, TIM-3), comprehensive macrophage phenotyping panels (eg, combining Iba-1, CD163 and CD204) and functional readouts to test these mechanisms in feline osteosarcoma specifically.

Age-related findings warrant a nuanced view. We observed a moderate negative correlation between age and $CD3^+$ and $CD8^+$ T cell densities, consistent with immunosenescence as reported in previous studies (Campbell *et al.,* 2004; Day, 2010; McKenzie, 2025). In addition, a previous study has shown that increased tumour-infiltrating T cells, particularly $CD8^+$ T cells, could be associated with worse outcomes in osteosarcoma patients (Palmerini *et al.*, 2017). This pattern supports a model in which 'quantity without quality' of T-cell infiltration, potentially compounded by age-linked functional decline, fails to translate into effective anti-tumour immunity. Longitudinal and mechanistic studies are needed to disentangle immune composition from competence across age strata in cats

Clinical implications remain preliminary. Our results suggest that, in feline osteosarcoma, higher $CD3^+$ T cell and $CD8^+$ T cell densities may flag an immune contexture enriched for dysfunctional or suppressed T cells, which could be relevant when considering immunotherapies (eg, checkpoint inhibitors or macrophage-modulating strategies). Before clinical adoption, these associations require external validation, harmonized scoring and integration with spatial and functional biomarkers.

This was a retrospective, single-centre subset analysis with a small sample size (n = 16). Immune densities were dichotomized by median split and multiple comparisons were not adjusted; Kaplan–Meier analyses were univariable, without control for potential

confounders (eg, anatomical site, metastatic status, treatments). Furthermore, due to the retrospective design and the lack of standardized post-operative restaging protocols, the precise timing of metastasis or recurrence could not be reliably determined; thus, overall survival was utilized as the primary robust endpoint rather than disease-free interval. Counts were derived from 10 random core fields by manual counting without formal statistical assessment of inter-observer repeatability and did not address spatial organisation (eg, the 'immune-excluded' phenotype, where immune cells accumulate at the tumour margin but fail to infiltrate the tumour core). Immune exclusion refers to a condition where effector immune cells are present in the TME but remain outside the tumour core, resulting in impaired anti-tumour activity (Tiwari *et al.*, 2023). These factors may inflate type-I error and limit generalizability, therefore our conclusions should be considered hypothesis generating.

Prospective studies with larger cohorts should (i) integrate spatial profiling (eg, multiplex IHC/immunofluorescence or spatial transcriptomics) to explicitly compare infiltrates in the central tumour versus the invasive margin, (ii) include checkpoint and exhaustion markers to assess T-cell quality, (iii) refine macrophage phenotyping beyond CD204 and (iv) apply multivariable survival models and appropriate multiplicity control. Such frameworks will better define whether feline osteosarcoma harbours an 'inflamed but suppressed' immune state and identify actionable pathways for therapy.

In summary, feline osteosarcomas in our series contained macrophage-rich, T-cell–infiltrated TMEs in which higher $CD3^+$ T cell and $CD8^+$ T cell densities were associated with a poorer clinical outcome and shorter OST. These data support the working hypothesis that T-cell infiltration may be present yet functionally constrained,

underscoring the need for spatial-functional immune profiling and external validation before prognostic use.

2.6 Conclusions

The results of this study indicate that high T-cell infiltration in feline osteosarcoma is associated with an unfavourable prognosis. This finding opens up opportunities for further research on the regulatory mechanisms of immune cells and immune checkpoints within the TME of feline osteosarcoma to determine prognosis and develop immunotherapy strategies.

2.7 Table of Chapter II

Table 2.1 Baseline clinical features of 16 cats with appendicular osteosarcoma.

Clinical features	
Age, (mean ± SD, year)	9.44 ± 5.02
Body weight, (mean ± SD, kg)	4.25 ± 1.79
Sex, n (%)	
Male	1 (6.25)
Female	2 (12.5)
Male castrated	6 (37.5)
Female spayed	7 (43.75)
Tumour location, n (%)	
Femur	6 (37.5)
Humerus	3 (18.75)
Radius	2 (12.5)
Tibia	2 (12.5)
Distal radius/ulna	2 (12.5)
Scapula	1 (6.25)
Clinical outcome, n (%)	
Dead	10 (62.5)
Alive	4 (25)
Unknown	2 (12.5)

Note: n = number of cases

Table 2.2 Correlation between tumour-infiltrating immune cells in 16 cats with appendicular osteosarcoma.

	$CD3^+$ T cells	$CD8^+$ T cells	$Foxp3^+$ Tregs	$CD20^+$ B cells	$CD204^+$ macrophages
$CD3^+$ T cells		0.9389	0.2914	0.3488	0.7147
		< 0.0001*	0.2734	0.1855	0.002*
$CD8^+$ T cells			0.3300	0.2758	0.6814
			0.2119	0.3012	0.004*
$Foxp3^+$ Tregs				0.4672	0.2531
				0.0680	0.3443
$CD20^+$ B cells					0.3971
					0.1277
$CD204^+$ macrophages					

The first and second rows show the Spearman's correlation (r) value and the corresponding *P* value for each variable, respectively. * $P < 0.05$.

2.8 Figures of Chapter II

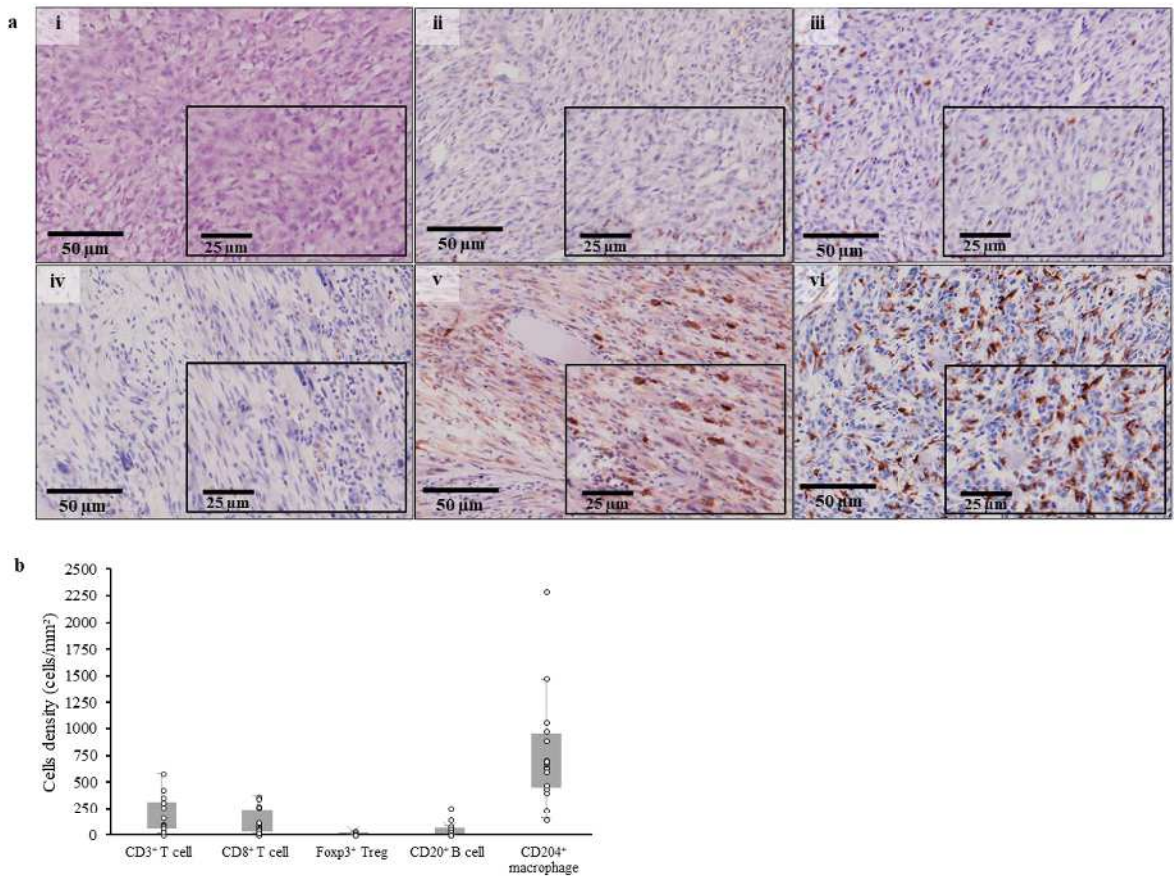


Figure 2.1 Tumour-infiltrating immune cells, feline appendicular osteosarcoma. (**a**) Representative HE and IHC (brown pigment): (**i**) HE, (**ii**) $CD3^+$ T cells, (**iii**) $CD8^+$ T cells, (**iv**) $Foxp3^+$ Tregs, (**v**) $CD20^+$ B cells and (**vi**) $CD204^+$ macrophages. 50 µm (main images) and 25 µm (insets). (**b**) Comparison of immune cell densities among subsets. Each dot represents the density in an individual case, and bars indicate interquartile range.

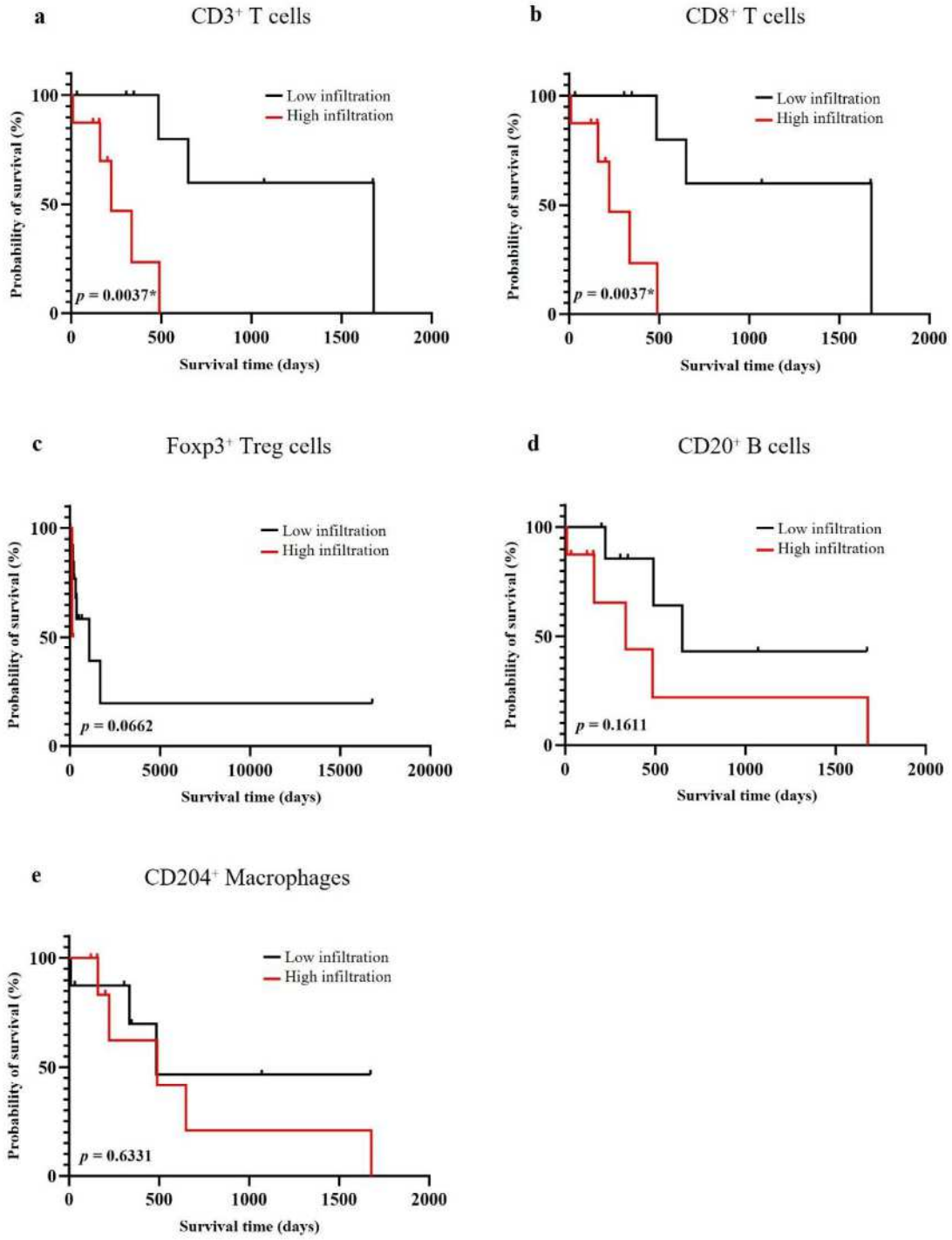


Figure 2.2 Kaplan–Meier survival curves comparing overall survival between 16 cats with appendicular osteosarcomas with high and low immune cell infiltration groups. Statistical significance was assessed using the log-rank test. Tick marks ("|") indicate censored observations.

GENERAL DISCUSSION

Tumour-infiltrating immune cells are key components of the tumour microenvironment and are known to influence tumour progression in both human and canine cancers. However, in feline tumour—particularly oral squamous cell carcinoma and osteosarcoma—studies investigating immune cell characteristics and their roles in tumour progression and survival remain limited. To improve clinical relevance, this study evaluated tumour-infiltrating immune cells for prognostic value in feline oral squamous cell carcinoma and osteosarcoma, to support future diagnostic and therapeutic strategies. Using immunohistochemistry, immune cell populations associated with survival outcomes were identified in both tumour types.

The first chapter focuses on immune cell infiltration in feline oral squamous cell carcinoma as a prognostic indicator. Although previous studies have described patterns of immune cell infiltration (Sparger *et al.,* 2018), their association with survival has not been established. In this study, $CD204^+$ macrophages were consistently observed in all samples, both within the tumour core and the stroma. A moderate negative correlation was identified between tumour $CD3^+$ T cell density and both progression-free interval (PFI) and overall survival time (OST). Similarly, stromal $CD20^+$ B cell density showed a moderate negative correlation with PFI. The Kaplan–Meier analysis further demonstrated that cases with lower tumour $CD3^+$ T cell infiltration had significantly longer OST than those with higher infiltration. In addition, lower stromal $CD8^+$ T cell infiltration was associated with significantly longer PFI and showed a tendency toward longer OST.

Chapter 2 examines feline osteosarcoma, a relatively rare tumour in which biological characteristics have been described (Dimopoulou *et al.,* 2008), but immune infiltration patterns and their prognostic significance remain unclear. Consistent with

findings in oral squamous cell carcinoma, $CD204^+$ macrophages were present in all cases and represented the most abundant immune cell population. Higher $CD3^+$ T cell density was significantly associated with vital status, while $CD8^+$ T cells and $CD204^+$ macrophages showed weaker associations. Kaplan–Meier analysis indicated that lower densities of $CD3^+$ and $CD8^+$ T cells were associated with longer overall survival.

These findings differ from several previous studies in human, canine, and feline tumours, which generally report a positive association between T cell infiltration and survival (Casanova *et al.*, 2021; Koirala *et al.*, 2016; Nascimento *et al.,* 2022; Razmara *et al*., 2021; Sales de Sá *et al.,* 2021; Suárez-Sánchez *et al*., 2021; Withers *et al*., 2019b; Wongpattaraworakul *et al.*, 2024). Although this study does not provide direct mechanistic evidence, several hypotheses may explain why higher T cell infiltration is associated with shorter survival in these feline tumours. First, the high abundance of $CD204^+$ macrophages suggests a potentially immunosuppressive microenvironment, in which macrophages may inhibit T cell function through the release of checkpoint ligands or immunoregulatory cytokines (Koirala *et al*., 2016; Kondo *et al.*, 2021; Kubota *et al.*, 2017; Luo *et al.*, 2020; Ruffell *et al.*, 2014; Tatsuno et al., 2024; Xue *et al*., 2022). Second, infiltrating T cells may be functionally exhausted, leading to a reduced anti-tumour immune response (Cheng *et al.*, 2024; Pauken and Wherry, 2015; Sun *et al.*, 2021). Additionally, this study did not evaluate spatial immune patterns, such as immune-excluded or diffusely infiltrated patterns, in which immune cells in the tumour core may not effectively control tumour growth (Tsujikawa *et al.*, 2020).

In summary, both studies on feline oral squamous cell carcinoma and osteosarcoma demonstrated abundant macrophage infiltration and higher densities of $CD3^+$ and $CD8^+$ T cells, which were associated with shorter survival. These findings

support the hypothesis that T cell infiltration may be present but functionally ineffective. Therefore, further investigation incorporating spatial and functional immune profiling, along with external validation, is necessary before these markers can be reliably used for prognostic purposes.

Acknowledgement

All praise and gratitude be to Allah SWT, the Almighty, for His endless blessings, guidance, and mercy that have enabled me to pursue and complete my doctoral study and research at the Laboratory of Molecular Diagnostics and Therapeutics, Joint Graduate School of Veterinary Medicine, Yamaguchi University, Yamaguchi, Japan. Peace and blessings be upon the Prophet Muhammad SAW, the greatest teacher and role model for all humankind.

With profound respect and gratitude, I would like to express my appreciation to Professor Takuya Mizuno, DVM, PhD, my main supervisor at the Laboratory of Molecular Diagnostics and Therapeutics, for his continuous guidance, encouragement, and invaluable support throughout my doctoral study. I am sincerely thankful for the opportunity he provided me to learn and participate in various laboratory and clinical activities at the Yamaguchi University Animal Medical Center.

My sincere appreciation goes to my doctoral thesis examiners, Professor Takeshi Kusakabe, PhD, DVM, Professor Kenji Tani, DVM, PhD, Professor Naoki Miura, DVM, PhD, Associate Professor Masaya Igase, DVM, PhD for their constructive sugesstions and thoughftful evaluation of my doctoral thesis. My sincere appreciation also goes to my co-supervisors, Associate Professor Kenji Baba, DVM, PhD, and Professor Yasuyuki Endo, DVM, PhD, for their kind advice, constructive feedback, and support during my research and study period. I would also like to express my sincere gratitude to Associate Professor Masaya Igase, DVM, PhD, Nishibori Shoma, DVM, Professor Masaru Okuda, DVM, PhD, and Satoshi Kambayashi, DVM, PhD, for their guidance, teaching, and valuable discussions during my training and collaborative work in the Laboratory of

Veterinary Internal Medicine, the Laboratory of Veterinary Clinical Pathology, and the Yamaguchi University Animal Medical Center.

My heartfelt thanks are extended to all members and technical staff of the Laboratory of Molecular Diagnostics and Therapeutics and the Laboratory of Internal Medicine for their cooperation, encouragement, and warm friendship during my study. I am also grateful to all veterinarians and staff members at North Lab, Sapporo, Hokkaido and the Japan Small Animal Cancer Center (affiliated with the Japan Small Animal Medical Center Foundation), Saitama, for their kind assistance and support in completing my doctoral research project.

I am truly grateful to the Ministry of Education, Culture, Sports, Science and Technology (MEXT), Japan, for providing me with the valuable opportunity and scholarship to study and conduct research at Yamaguchi University.

I also extend my gratitude to my lecturers, colleagues, and all members of the Division of Internal Medicine, School of Veterinary Medicine and Biomedical Sciences, IPB University, Indonesia, for their continuous prayers, support, and encouragement throughout my academic journey.

My deepest appreciation goes to my beloved family–Rini Septiani and Alhazen Miqhad Badruzzaman–for their endless love, patience, and prayers. I am equally indebted to my beloved parents and parents-in-law for their constant encouragement and heartfelt prayers. Finally, I thank all my friends and everyone who has contributed, directly or indirectly, to the completion of this dissertation. May this work bring benefit and contribute to the advancement of veterinary medical science.

Arief Purwo Mihardi

REFERENCES

1. Abd Elmoneim HM, Huwait HF, Nafady-Hego H, Mohamed FA. Prognostic implications of PD-L1 expression and loss of PTEN in patients with rhabdomyosarcoma, ewing's sarcoma and osteosarcoma. *Exp Oncol* 2023; 45(3): 337-350.
2. Barbosa AM, Mantinho O, Nogueira R, Campos J, Lobo L, Pinto H, *et al.* Increased $CD3^+$, $CD8^+$, or $Foxp3^+$ T lymphocyte infiltrations are associated with the pathogenesis of colorectal cancer but not with the overall survival of patients. *Biology* 2021; 10(8): 808.
3. Berntsson J, Nodin B, Eberhard J, Micke P, Jirström K. Prognostic impact of tumour-infiltrating B cells and plasma cells in colorectal cancer. *Int J Cancer* 2016; 139(5): 1129-39.
4. Binnewies M, Roberts EW, Kersten K, Chan V, Fearon DF, Merad M, *et al.* Understanding the tumor immune microenvironment (TIME) for effective therapy. *Nat Med* 2018; 24(5): 541-50.
5. Bjørland K, Flatmark K, Pettersen S, Aaasen AO, Fodstad O, Maelandsmo GM. Matrix metalloproteinases participate in osteosarcoma invasion. *J Surg Res* 2005; 127(2): 151-156.
6. Boss MK, Harrison LG, Gold A, Karam SD, Regan DP. Canine oral squamous cell carcinoma as a spontaneous, translational model for radiation and immunology research. *Front Oncol* 2023; 12: 1033704.

7. Boston SE, Ehrhart NP, Dernell WS, Lafferty M, Withrow SJ. Evaluation of survival time in dogs with stage III osteosarcoma that undergo treatment: 90 cases (1985-2004). *J Am Vet Med Assoc* 2006; 228(12): 1905-1908.

8. Campbell DJ, Rawlings JM, Koelsch S, Wallace J, Strain JJ, Hannigan BM. Age-related differences in parameters of feline immune status. *Vet Immunol Immunopathol* 2004; 100(1-2): 73-80.

9. Caruntu A, Moraru L, Lupu M, Vasilescu F, Dumitrescu M, Ciplea M, *et al.* Progonostic potential of tumor-infiltrating immune cells in resectable oral squamous cell carcinoma. *Cancers* 2021; 13(9): 2268.

10. Casanova JM, Almeida JS, Reith JD, Sousa LM, Fonseca R, Fretas-Tavares P, *et al. Tumor*-infiltrating lymphocytes and cancer markers in osteosarcoma: influence on patient survival. *Cancers* 2021; 13(23): 6075.

11. Chaudhari N, Prakash N, Pradeep GL, Mahajan A, Lunawat S, Salunkhe V. Evaluation of density of tumor-associated macrophages using CD163 in histological grades of oral squamous cell carcinoma, an immunohistochemical study. *J Oral Maxillofac Pathol* 2021; 24(3): 577.

12. Chen CW, Wang HC, Tsai IM, Chen IS, Chen CJ, Hou YC, *et al.* CD204-positive M2-like tumor-associated macrophages increase migration of gastric cancer cells by upregulating miR-210 to reduce NTN4 expression. *Cancer Immunol Immunother* 2024; 73(1): 1.

13. Cheng D, Zhang Z, Liu D, Mi Z, Tao W, Fu J, Fan H. Unraveling T cell exhaustion in the immune microenvirontment of osteosarcoma via single-cell RNA transcriptome. *Cancer Immunol Immunother* 2024; 73(2): 35.

14. Cray M, Selmic LE, Ruple A. Demographics of dogs and cats with oral tumors presenting to teaching hospitals: 1996-2017. *J Vet Sci* 2020; 21(5): e70.

15. Dagher E, Simbault L, Abadie J, Loussouarn D, Campone M, Nguyen F. Identification of an immune-suppressed subtype of feline triple-negative basal-like invasive mammary carcinomas, spontaneous models of breast cancer. *Tumor Biol* 2020; 42(1): 1010428319901052.

16. Day MJ. Ageing, immunosenescence and inflammageing in the dog and cat. *J Comp Pathol* 2010; 142 Suppl1: S60-S69.

17. Dimopoulou M, Kirpensteijn J, Moens H, Kik M. Histologic prognosticators in feline osteosarcoma: a comparison with phenotypically similar canine osteosarcoma. *Vet Surg* 2008; 37(5): 466-71.

18. Ding Z, Li Y, Zhong C. Integrated RNA sequencing reveals tumor microenvironment heterogeneity and immunosuppressive role of M2 macrophages in osteosarcoma. *Oncologie* 2025;27(5): 759–78.

19. Edin S, Kaprio T, Haström J, Larsson P, Mustonen H, Böckelman C, *et al.* The prognostic importance of $CD20^{+}$ B lymphocytes in colorectal cancer and the Relation to other immune cell subsets. *Sci Rep* 2019; 9(1): 19997.

20. Fang J, Li X, Ma D, Liu X, Chen Y, Wang Y, *et al.* Prognostic significance of tumor infiltrating immune cells in oral squamous cell carcinoma. *BMC Cancer* 2017; 17(1): 375.

21. Flecher MC, Reys MP, Balabram D, Nakagaki KYR, Cassali GD. Tumor-infiltrating lymphocytes and neutrophils and their location in canine mammary neoplasms with a solid arrangement: a prognostic factor?. *Animals* 2025; 15(2): 287.

22. Fujii N, Shomori K, Shiomi T, Nakabayashi M, Takeda C, Ryoke K, *et al.* Cancer-associated fibroblasts and CD163-positive macrophages in oral squamous cell carcinoma: their clinicopathological and prognostic significance. *J Oral Pathol Med* 2012; 41(6): 444-451.

23. Fritzsching B, Fellenberg J, Moskovszky L, Sápi Z, Krenacs T, Machado I, *et al*. $CD8^+/FOXP3^+$-ratio in osteosarcoma microenvironment separates survivors from non-survivor: a multicenter validated retrospective study. *Oncoimmunology* 2015; 4(3): e990800.

24. Gajewski TF, Schreiber H, Fu YX. Innate and adaptive immune cells in the tumor microenvironment. *Nat Immuno* 2013; 14(10): 1014-22.

25. Gentles AJ, Newman AM, Liu CL, Bratman SV, Feng W, Kim D, *et al.* The prognostic landscape of genes and infiltrating immune cells across human cancers. *Nat Med* 2015; 21(8): 938-45.

26. Giraldo NA, Peske JD, Sautès-Fridman C, Fridman WH. Integrating histopathology, immune biomarkers, and molecular subgroups in solid cancer: the next step in precision oncology. *Virchows Arch* 2019; 474(4): 463-74.

27. Gooden MJM, de Bock GH, Leffers N, Daemen T, Nijman HW. The prognostic influence of tumour-infiltrating lymphocytes in cancer: a systematic review with meta-analysis. *Br J Cancer* 2011; 105(1): 93-103.

28. Guangning Y, Ling Y, Xuwen L, Danli Y, Wei W, Zhuocai W. Correlation between PD-1/CTLA-4 expression with clinicopathological features and prognosis of osteosarcoma patients. *Cancer Res Prev Treat* 2023; 50(1): 63-68.

29. Hashimoto K, Nishimura S, Akagi M. Characterization of PD-1/PD-L1 immune checkpoint expression in osteosarcoma. *Diagnostics* 2020; 10(8): 528.

30. Heldmann E, Anderson MA, Wagner-Mann C. Feline osteosarcoma: 145 cases (1990-1995). *J Am Anim Hosp Assoc* 2000; 36(6): 518-21.

31. Hu C, Liu C, Tian S. Comprehensive analysis of prognostic tumor microenvironment-related genes in osteosarcoma patients. *BMC Cancer* 2020; 20(1): 814.

32. Huber D, Severin K, Vlahović D, Križanac S, Mofardin S, Buhin IM, et al. Cancer morbidity in Croatian cats: retrospective study on spontaneously arising tumors (2009-2019). *Top Companion Anim Med* 2024; 58: 100841.

33. Iwata T, Ichimata M, Fujita A, Shiraishi Y, Kagawa Y, Toshima A, *et al*. The outcome and surgical complications of cats with oral squamous cell carcinoma treated with total glosso-mandibulectomy: 20 cases (2008-2022). *Vet Comp Oncol* 2025; 23(2): 178-86.

34. Joudžiukynienė N. Retrospective analysis of prevalence of tumors in dogs and cats in Lithuania. *Vet Sci* 2025; 12: 1038.

35. Kahdeh H, Derakhshanfar G, Mehr OR. Evaluation of tumor-associated macrophages and micro-vessel density in verrucous carcinoma and squamous cell carcinoma of the oral cavity. *Adv Biomed Res* 2024; 13: 67.

36. Kasurinen J, Hagström J, Kaprio T, Lehtonen IB, Haglund C, Böckelman C. Tumor-associated CD3- and CD8-positive immune cells in colorectal cancer: The additional prognostic value of $CD8^+$-to-$CD3^+$ ratio remains debatable. *Tumour Biol* 2022; 44(1): 37-52.

37. Kent MS, Karchemskiy S, Culp WTN, Lejeune AM, Pesavento PA, Toedebusch C, et al Longevity and mortality in cats: a single institution necropsy study of 3108 cases (1989-2019). *PLoS ONE* 2022; 17(12): e0278199

38. Koirala P, Roth ME, Gill J, Piperdi S, Chinai JM, Geller DS, *et al.* Immune infiltration and PD-L1 expression in the tumor microenvironment are prognostic in osteosarcoma. *Sci Rep* 2016; 6: 30093.

39. Kondo Y, Suzuki S, Takahara T, Ono S, Goto M, Miyabe S, *et al*., Improving function of cytotoxic T-lymphocytes by transforming growth factor-β inhibitor in oral squamous cell carcinoma. *Cancer Sci* 2021; 112(10): 4037-49.

40. Kubota K, Moriyama M, Furukawa S, Rafiul HASM, Maruse Y, Jinno T, *et al.* $CD163^+$ $CD204^+$ tumor-associated macrophages contribute to T cell regulation via interleukin-10 and PD-L1 production in oral squamous cell carcinoma. *Sci Rep* 2017;7(1): 1755.

41. Laissaoui N, Millán Y, Bets DS, Mrini ME, Lamalmi N, Azrib R, et al. Evaluation of canine and feline tumors in Morocco: result of a prospective observational study of 250 cases (2020-2023). *Top Companion Anim Med* 2024; 63: 100929.

42. Liang H, Cui M, Tu J, Chen X. Advancements in osteosarcoma management: integrating immune microenvironment insights with immunotherapeutic strategies. *Front Cell Dev Biol* 2024; 12: 1394339.

43. Ligon JA, Choi W, Cojocaru G, Fu W, Hsiue EHC, Oke TF, *et al.* Pathways of immune exclusion in metastatic osteosarcoma are associated with inferior patient outcomes. *J Immunother Cancer* 2021; 9(5): e001772.

44. Li HX, Wang SQ, Lian ZX, Deng SL, Yu K. Relationship between tumor infiltrating immune cells and tumor metastasis and its prognostic value in cancer. *Cells* 2022; 12(1): 64.

45. Liptak JM, Thatcher GP, Mestrinho LA, Séguin B, Vernier T, Martano M, *et al.* Outcome of cats treated with maxillectomy: 60 cases. a veterinary society of surgical oncology retrospective study. *Vet Comp Oncol* 2021; 19(4): 641-50.

46. Liu P, Xiao Q, Zhou B, Dai Z, Kang Y. Prognostic significance of programmed death ligand 1 expression and tumor-infiltrating lymphocytes in axial osteosarcoma. *World Neurosurg* 2019; 129: e240-e254.

47. Liu SK, Dorfman HD, Patnaik AK. Primary and secondary bone tumours in the cat. *J Small Anim Pract* 1974; 15(3): 141-56.

48. Liu W, Chen G, Zhang C, Liao X, Xie J, Liang T*, et al*. Prognostic significance of tumor-infiltrating lymphocytes and macrophages in nasopharyngeal carcinoma: a systematic review and meta-analysis. *Eur Arch Otorhinolaryngol* 2022; 279(1): 25-35.

49. Liu X, Wu S, Yang Y, Zhao M, Zhu G, Hou Z, *et al.* The prognostic landscape of tumor-infiltrating immune cell and immunomodulators in lung cancer. *Biomed Pharmacother* 2017; 95: 55-61.

50. Luo ZW, Liu PP, Wang ZX, Chen CY, Xie H. Macrophages in osteosarcoma immune microenvironment: implications for immunotherapy. *Front Oncol* 2020; 10: 586580.

51. Lv B, Wang Y, Ma D, Cheng W, Liu J, Yong T, *et al.* Immunotherapy: reshape the tumor immune microenvironment. *Front Immunol* 2022; 13:844142.

52. Mandara MT, Giglia G, Benedetti G, Falzone C, Balducci F, Pitzorno I, et al. Tumor-associated macrophages in feline meningiomas: Exploring their prognostic significance. *J Neuropathol Exp Neurol* 2025; 85(3): 220-227.

53. Mannheimer JD, Tawa G, Gerhold D, Braisted J, Sayers CM, McEachron TA, *et al.* Transcriptional profiling of canine osteosarcoma identifies prognostic gene expression signatures with translational value for humans. *Commun Biol* 2023; 6(1): 856.

54. Marconato L, Annoni M, Massari F, Zanardi S, Stefanello D, Ferrari R, *et al.* A retrospective Italian Society of Veterinary Oncology (SIONCOV) study of 56 cats with appendicular osteosarcoma. *Vet Comp Oncol* 2024; 22(2): 198-203.

55. McKenzie BA. Immunosenescence and inflammaging in dogs and cats: a narrative review. *J Vet Intern Med* 2025; 39(4): e70159.

56. Mihardi AP, Nururrozi A, Ichimata M, Kagawa Y, Igase M, Mizuno T. Investigation of tumour-infiltrating immune cells as a prognostic factor in feline oral squamous cell carcinoma. *J Comp Pathol* 2025; 223-9.

57. Mikiewicz M, Czapula KP, Gesek M, Lemishevskyi V, Domagala IO. Canine and feline oral cavity tumours and tumour-like lesions: a retrospective study of 486 cases (2015-2017). *J Comp Pathol* 2019; 172: 80-87.

58. Miyasato Y, Shiota T, Koji O, Pan C, Yano H, Horlad H *et al.* High density of CD204-positive macrophages predicts worse clinical prognosis in patients with breast cancer. *Cancer Sci* 2017; 108(8): 1693-1700.

59. Modiano JF, Bellgrau D, Cutter GR, Lana SE, Ehrhart NP, Ehrhart E, *et al.* Inflammation, apoptosis, and necrosis induced by neoadjuvant fas ligand gene therapy improves survival of dogs with spontaneous bone cancer. *Mol Ther* 2012; 20(12): 2234-43.

60. Mukherjee G, Bag S, Chakraborty P, Dey D, Roy S, Jain P, *et al.* Density of $CD3^+$ and $CD8^+$ cells in gingivo-buccal oral squamous cell carcinoma is associated with lymph node metastases and survival. *PLoS One* 2020; 15(11): e0242058.

61. Nakano Y, Kagawa Y, Shimoyama Y, Yamagami T, Nomura K, Wakabayashi H, *et al.* Outcome of appendicular or scapular osteosarcoma treated by limb amputation in cats: 67 cases (1997-2018). *J Am Vet Med Assoc* 2022; 260(S1): S24-S28.

62. Nascimento C, Gameiro A, Correia J, Ferreira J, Ferreira F. The landscape of tumor-infiltrating immune cells in feline mammary carcinoma: pathological and clinical implications. *Cells* 2022; 11(16): 2578.

63. Palmerini E, Agostinelli C, Picci P, Pileri S, Marafioti T, Lollini PL, *et al.* Tumoral immune-infiltrate (IF), PD-L1 expression and role of CD8/TIA-1 lymphocytes in localized osteosarcoma patients treated within protocol ISG-OS1. *Oncotarget* 2017; 8(67): 111836-111846

64. Pauken KE, Wherry EJ. Overcoming T cell exhaustion in infection and cancer. *Trends Immunol* 2015; 36(4): 265-76.

65. Pérez-Enriquez JM, Romero-Romero L, Alonso-Morales RA, Fuentes-Pananá EM. Tumor prevalence in cats: experience from a reference diagnostic center in Mexico City (2006-2018). *Vet Mex OA* 2020;7(4).

66. Perri F, Lonna F, Longo F, Scarpati GDV, Angelis CD, Ottaiano A, *et al*. Immune response against head and neck cancer: biological mechanisms and implication on therapy. *Transl Oncol* 2020;13(2): 262-74.

67. Piersiala K, Hjalmarsson E, Lagebro V, Neves da Silva PF, Bark R, Elliot A, *et al.* Prognostic value of T regulatory cells and immune checkpoints expression in

tumor-draining lymph nodes for oral squamous cell carcinoma. *Front Immunol* 2024; 15: 1455426.

68. Pinard CJ, Lagree A, Lu FI, Klein J, Oblak ML, Salgado R. Comparative evaluation of tumor-infiltrating lymphocytes in companion animals: immuno-oncology as a relevant translational model for cancer therapy. *Cancer* 2022; 14(20): 5008.

69. Porcellato I, Silvestri S, Sforna M, Banelli A, Giudice AL, Mechelli L, *et al*. Tumor-infiltrating lymphocytes (TILS) in feline melanocytic tumors: preliminary investigation. *Vet Immunol Immunopathol* 2021; 242: 110337.

70. Quigley PJ and Leedale AH. Tumors involving bone in the domestic cat: a review of fifty-eight cases. *Vet Pathol* 1983; 20(6): 670-86.

71. Rafiul HASM, Moriyama M, Kubota K, Ishiguro N, Sakamoto M, Chinju A, *et al.* $CD206^+$ tumor-associated macrophages promote proliferation and invasion in oral squamous cell carcinoma via EGF production. *Sci Rep* 2019; 9(1): 14611.

72. Razmara AM, Judge SJ, Gingrich AA, Cruz SM, Culp WTN, Kent MS, *et al.* Natural killer and T cell infiltration in canine osteosarcoma: clinical implications and translational relevance. *Front Vet Sci* 2021; 8: 771737.

73. Rissi DR, Porter BF, Boudreau CE, Krimer PM, Miller AD. Immunohistochemical characterization of immune cell infiltration in feline glioma. *J Comp Path* 2018; 160: 15-22.

74. Rossi A, Belmonte B, Carnevale S, Liotti A, Rosa VD, Jaillon S, *et al.* Stromal and immune cell dynamics in tumor associated tertiary lymphoid structures and anti-tumor immune responses. *Front Cell Dev Biol* 2022; 10: 933113.

75. Ruffell B, Chang-Strachan D, Chan V, Rosenbusch A, Ho CMT, Pryer N, *et al*. Macrophage IL-10 blocks $CD8^+$ T cells-dependent responses to chemotherapy by suppressing IL-12 expression in intratumoral dendritic cells. *Cancer Cell* 2014; 26(5): 623-637.

76. Sakai O, Li T, Uchida K, Igase M, Mizuno T. Establisment and characterization of monoclonal antibody against canine CD8 alpha. *Monoclon Antib Immunodiagn Immunother* 2020; 39(4): 129-34.

77. Sales de Sá R, Galvis MM, Mariz BALA, Leite AA, Schultz L, Almeida OP, *et al.* Increased tumor immune microenvironment $CD3^+$ and $CD20^+$ lymphocytes predict a better prognosis in oral tongue squamous cell carcinoma. *Front Cell Dev Biol* 2021; 8: 622161.

78. Seung BJ, Bae MK, Sur JH. Regional variations in and key predictors of feline tumor malignancy: a decade-long retrospective study in Korea. *Animals* 2024; 14(20): 2989.

79. Shaopeng Z, Yang Z, Yuan F, Chen H, Zhengjun Q. Regulation of regulatory T cells and tumor- associated macrophages in gastric cancer tumor microenvironment. *Cancer Med* 2024; 13(2): e6959.

80. Soltero-Rivera MM, Krick EL, Reiter AM, Brown DC, Lewis JR. Prevalence of regional and distant metastasis in cats with advanced oral squamous cell carcinoma: 49 cases (2005-2011). *J Feline Med Surg* 2014;16(2): 164-169.

81. Sparger EE, Murphy BG, Kamal FM, Arzi B, Nadyan D, Skouritakis CT, *et al.* Investigation of immune cell markers in feline oral squamous cell carcinoma. *Vet Immunol Immunopathol* 2018; 202: 52-62.

82. Stebbins KE, Morse CC, Goldschmidt MH. Feline oral neoplasia: a ten-year survey. *Vet Pathol.* 1989;26(2):121–4.

83. Strohmayer C, Klang A, Kneissl S. Computed tomographic and histopathological characteristics of 13 equine and 10 feline oral and sinonasal squamous cell carcinomas. *Front Vet Sci* 2020; 7: 591437.

84. Suárez-Sánchez FJ, Lequerica-Fernández P, Rodrigo JP, Hermida-Prado F, Suárez-Canto J, Rodríguez-Santamarta T, *et al.* Tumor-infiltrating CD20+ B lymphocytes: significance and prognostic implications in oral cancer microenvironment. *Cancers* 2021; 13(3): 395.

85. Sun CY, Zhang Z, Tao L, Xu FF, Li HY, Zhang HY, *et al.* T cell exhaustion drives osteosarcoma pathogenesis. *Ann Transl Med* 2021; 9(18): 1447.

86. Surendran S, Aboelkheir W, Tu AA, Magner WJ, Sigurdson SL, Merzianu M, *et al.*, T-cell infiltration and immune checkpoint expression increase in oral cavity premalignant and malignant disorders. *Biomedicines* 2022; 10(8): 1840.

87. Tang D, Tao D, Fang Y, Deng C, Xu Q, Zhou J. TNF-alpha promotes invasion and metastasis via NF-Kappa B pathway in oral squamous cell carcinoma. *Med Sci Monit Basic Res* 2017; 23: 141-9.

88. Tatsuno R, Komohara Y, Pan C, Kawasaki T, Enomoto A, Jubashi T, et al. Surface markers and chemokines/cytokines of tumor-associated macrophages in osteosarcoma and other carcinoma microenvironments-contradictions and comparisons. *Cancers* 2024;16(16): 2801.

89. Tauriello DVF, Palomo-Ponce S, Stork D, Berenguer-Llergo A, Badia-Ramentol J, Iglesias M, *et al*. TGFβ drives immune evasion in genetically reconstituted colon cancer metastasis. *Nature* 2018; 554(7693): 538-543.

90. Tiwari A, Oravecz T, Dillon LA, Italiano A, Audoly L, Fridman WH, et al. Towards a consensus definition of immune exclusion in cancer. *Front Immunol* 2023; 14: 1084887.

91. Tsujikawa T, Mitsuda J, Ogi H, Hayashino AM, Konishi E, Itoh K, et al. Prognostic significance of spatial immune profiles in human solid cancers. *Cancer Sci* 2020;111(10): 3426–34.

92. Wongpattaraworakul W, Choi A, Buchakjian MR, Lanzel EA, Kd AR, Simons AL. Prognostic role of tumor-infiltrating lymphocytes in oral squamous cell carcinoma. *BMC Cancer* 2024; 24: 766.

93. Withers SS, Skorupski KA, York D, Choi JW, Woolard KD, Laufer-Amorim R, *et al.* Association of macrophage and lymphocyte infiltration with outcome in canine osteosarcoma. *Vet Comp Oncol* 2019a; 17(1): 49-60.

94. Withers SS, York D, Choi JW, Woolard KD, Laufer-Amorim R, Sparger EE, *et al.* Metastatic immune infiltrates correlate with those of the primary tumour in canine osteosarcoma. *Vet Comp Oncol* 2019b; 17(3): 242-252.

95. Xia Q, Jia J, Hu C, Lu J, Li J, Xu H, *et al.* Tumor-associated macrophages promote PD-L1 expression in tumor cells by regulating PKM2 nuclear translocation in pancreatic ductal adenocarcinoma. *Oncogene* 2021; 41(6): 865-877.

96. Xie Y, Tang G, Xie P, Zhao X, Chen C, Li X, *et al.* High $CD204^{+}$ tumor-associated macrophage density predicts a poor prognosis in patients with clear cell renal cell carcinoma. *J Cancer* 2024; 15(6): 1511-22.

97. Xue Y, Song X, Fan S, Deng R. The role of tumor-associated macrophages in oral squamous cell carcinoma. *Front Physiol* 2022; 13: 959747.

98. Yamagata Y, Tomioka H, Sakamoto K, Sato K, Harada H, Ikeda T, *et al*. CD163-positive macrophages within the tumor stroma are associated with lymphangiogenesis and lymph node metastasis in oral squamous cell carcinoma. *J Oral Maxillofac Surg* 2017; 75(10): 2144-53.

99. Yang B, Su Z, Chen G, Zeng Z, Tan J, Wu G, *et al.* Identification of prognostic biomarkers associated with metastasis and immune infiltration in osteosarcoma. *Oncol Lett* 2021; 21(3): 180.

100. Ye L, Zhang T, Kang Z, Guo G, Sun Y, Lin K, *et al.* Tumor-infiltrating immune cells act as a marker for prognosis in colorectal cancer. *Front Immunol* 2019; 10: 2368.

101. Yokota S, Kaji K, Yonezawa T, Momoi Y, Maeda S. $CD204^{+}$ tumor-associated macrophages are associated with clinical outcome in canine pulmonary adenocarcinoma and transitional cell carcinoma. *Vet J* 2023; 296-297: 105992.

102. Yuen GJ, Demissie E, Pillai S. B lymphocytes and cancer: a love-hate relationship. *Trends Cancer* 2016; 2(12): 747-757.

103. Zaccone R, Renzi A, Chalfon C, Lenzi J, Bellei E, Marconato L, *et al*. Environmental risk factors for the development of oral squamous cell carcinoma in cats. *J Vet Intern Med* 2021; 36(4): 1398-408.

104. Zhang D, Tang D, Heng Y, Zhu XK, Zhou L, Tao L, *et al*. Prognostic impact of tumor-infiltrating lymphocytes in laryngeal squamous cell carcinoma patients. *Laryngoscope* 2021; 131(4): E1249-55.

105. Zhou Z, Wang J, Wang J, Yang S, Wang R, Zhang G, et al. Deciphering the tumor immune microenvironment from a multidimensional omics perspective: insight

into next-generation CAR-T cell immunotherapy and beyond. *Mol Cancer* 2024;23(1): 131.

106. Zou R, Gu R, Yu X, Hu Y, Yu J, Xue X, *et al.* Characteristics of infiltrating immune cells and a predictive immune model for cervical cancer. *J Cancer* 2021; 12(12): 3501-14.

APPENDICES

Supplementary Table 1. Tumour-infiltrating immune cell density in each feline oral squamous cell carcinoma case.

Case number	Tumour infiltrating immune cell density (cells/mm²)									
	CD3⁺ T cells		CD8⁺ T cells		CD20⁺ B cells		Foxp3⁺ Tregs		CD204⁺ macrophages	
	Stroma	Tumour	Stroma	Tumour	Stroma	Tumour	Stroma	Tumour	Stroma	Tumour
1	62.91 ± 28.16	55.5 ± 43.35	13.14 ± 22.15	1.37 ± 4.34	30.43 ± 10.51	4.41 ± 9.46	0.00 ± 0.00	0.00 ± 0.00	48.05 ± 27.47	65.75 ± 51.49
2	35.05 ± 12.84	15.22 ± 13.94	14.75 ± 14.40	6.23 ± 8.78	20.73 ± 13.41	0.00 ± 0.00	0.00 ± 0.00	0.00 ± 0.00	41.85 ± 19.62	54.13 ± 38.14
3	60.94 ± 53.26	11.77 ± 11.27	10.62 ± 11.92	0.00 ± 0.00	63.30 ± 37.33	0.00 ± 0.00	0.00 ± 0.00	0.00 ± 0.00	41.25 ± 27.31	14.16 ± 9.96
4	38.59 ± 37.38	30.86 ± 68.78	10.96 ± 30.68	0.00 ± 0.00	35.84 ± 17.06	0.00 ± 0.00	0.00 ± 0.00	0.00 ± 0.00	71.61 ± 24.81	40.21 ± 27.58
5	35.31 ± 24.59	73.65 ± 74.27	0.00 ± 0.00	0.00 ± 0.00	8.58 ± 6.46	0.00 ± 0.00	0.00 ± 0.00	0.00 ± 0.00	58.18 ± 43.17	37.00 ± 33.21
6	334.16 ± 177.60	74.02 ± 49.72	138.32 ± 96.22	69.57 ± 43.24	257.02 ± 200.59	0.00 ± 0.00	0.00 ± 0.00	0.00 ± 0.00	20.16 ± 15.88	4.52 ± 5.75
7	0.00 ± 0.00	0.00 ± 0.00	0.00 ± 0.00	0.00 ± 0.00	0.00 ± 0.00	0.00 ± 0.00	0.00 ± 0.00	0.00 ± 0.00	57.28 ± 49.85	13.38 ± 4.38
8	189.88 ± 233.29	77.69 ± 37.56	12.97 ± 18.25	16.62 ± 24.95	133.64 ± 158.46	35.94 ± 97.96	0.00 ± 0.00	0.00 ± 0.00	96.56 ± 33.92	111.46 ± 40.31
9	125.00 ± 108.89	34.49 ± 50.68	25.72 ± 43.40	9.51 ± 19.38	48.14 ± 50.12	8.74 ± 20.35	44.79 ± 57.02	1.23 ± 3.88	409.80 ± 315.22	66.15 ± 55.82
10	732.89 ± 577.42	342.70 ± 284.56	280.69 ± 234.96	367.48 ± 349.32	129.97 ± 64.57	30.19 ± 15.46	46.23 ± 67.80	9.57 ± 12.75	272.59 ± 82.88	211.4 ± 91.07
11	25.85 ± 14.60	0.00 ± 0.00	0.00 ± 0.00	0.00 ± 0.00	13.62 ± 12.00	0.00 ± 0.00	0.00 ± 0.00	0.00 ± 0.00	35.66 ± 29.94	9.23 ± 12.65
12	51.80 ± 57.38	103.70 ± 172.21	21.11 ± 30.05	5.19 ± 13.54	38.65 ± 53.64	9.76 ± 30.85	0.00 ± 0.00	0.00 ± 0.00	77.62 ± 53.16	31.94 ± 20.57
13	221.63 ± 88.32	315.10 ± 155.45	121.88 ± 58.37	375.12 ± 286.63	28.9 ± 28.30	0.00 ± 0.00	143.14 ± 112.35	74.14 ± 44.85	193.37 ± 57.23	267.71 ± 146.26
14	24.67 ± 23.61	13.09 ± 25.07	0.00 ± 0.00	0.00 ± 0.00	21.05 ± 17.73	0.00 ± 0.00	0.00 ± 0.00	0.00 ± 0.00	27.48 ± 30.33	18.06 ± 17.06
15	52.22 ± 50.42	18.47 ± 21.85	29.12 ± 15.68	15.74 ± 20.09	49.60 ± 51.53	1.03 ± 3.26	0.00 ± 0.00	0.00 ± 0.00	53.16 ± 24.54	55.69 ± 30.63
16	85.16 ± 119.01	91.28 ± 113.43	16.69 ± 34.50	0.00 ± 0.00	40.80 ± 41.51	0.00 ± 0.00	0.00 ± 0.00	0.00 ± 0.00	10.9 ± 6.52	10.07 ± 14.77
17	193.24 ± 195.97	76.17 ± 85.34	34.11 ± 39.19	10.02 ± 15.52	194.74 ± 213.17	4.13 ± 5.72	76.25 ± 50.67	8.50 ± 12.37	409.73 ± 132.91	206.1 ± 85.17
18	838.36 ± 486.95	386.07 ± 242.10	386.84 ± 241.23	270.69 ± 154.57	174.22 ± 108.99	33.84 ± 53.00	306.29 ± 280.59	36.22 ± 35.74	225.59 ± 94.96	96.35 ± 35.95
19	5.88 ± 4.65	20.51 ± 33.09	2.94 ± 6.35	0.00 ± 0.00	33.97 ± 19.34	4.83 ± 15.29	0.00 ± 0.00	0.00 ± 0.00	19.5 ± 10.17	44.43 ± 26.57
20	48.86 ± 26.01	25.21 ± 33.65	7.18 ± 5.14	0.00 ± 0.00	32.54 ± 13.52	0.00 ± 0.00	0.00 ± 0.00	0.00 ± 0.00	33.07 ± 12.72	73.88 ± 41.71
Average (Range, cells/mm²)	**158.12 (0.00 - 838.36)**	**88.27 (0.00 - 386.07)**	**56.35 (0.00 - 386.84)**	**57.38 (0.00 - 375.12)**	**67.79 (0.00 - 257.02)**	**6.64 (0.00 - 35.94)**	**30.83 (0.00 - 306.29)**	**6.48 (0.00 - 74.14)**	**110.17 (10.9 - 409.8)**	**71.58 (4.52 - 267.71)**

Supplementary Table 2. Tumour-infiltrating immune cells density in each cat with appendicular osteosarcoma case

Case number	Tumour-infiltrating immune cells density (cells/mm^2)				
	$CD3^+$ T cells	$CD8^+$ T cells	$Foxp3^+$ Tregs	$CD20^+$ B cells	$CD204^+$ macrophages
1	84.66 ± 10.93	0.00 ± 0.00	0.00 ± 0.00	32.04 ± 7.45	661.39 ± 99.36
2	87.59 ± 5.87	65.88 ± 9.80	0.00 ± 0.00	77.98 ± 7.74	1,549.52 ± 187.66
3	444.79 ± 36.37	379.44 ± 21.10	0.00 ± 0.00	28.20 ± 6.37	2,408.84 ± 199.83
4	90.57 ± 3.44	86.57 ± 3.10	0.00 ± 0.00	43.50 ± 4.73	661.65 ± 56.98
5	29.28 ± 6.42	22.57 ± 5.56	0.00 ± 0.00	0.00 ± 0.00	449.04 ± 56.09
6	317.25 ± 58.98	275.10 ± 69.37	38.97 ± 8.99	152.10 ± 48.68	1,022.15 ± 97.57
7	0.00 ± 0.00	0.00 ± 0.00	0.00 ± 0.00	0.00 ± 0.00	240.53 ± 21.03
8	273.71 ± 8.18	106.81 ± 7.52	0.00 ± 0.00	258.62 ± 13.59	620.90 ± 11.61
9	368.89 ± 29.03	280.95 ± 18.98	0.00 ± 0.00	0.00 ± 0.00	701.02 ± 87.38
10	604.03 ± 86.76	355.36 ± 31.37	0.00 ± 0.00	0.00 ± 0.00	934.86 ± 72.62
11	81.47 ± 10.99	54.85 ± 7.68	0.00 ± 0.00	18.38 ± 4.48	739.31 ± 56.21
12	164.57 ± 53.17	117.66 ± 37.71	11.14 ± 7.56	53.02 ± 10.79	733.26 ± 98.93
13	105.22 ± 11.28	67.98 ± 8.70	0.00 ± 0.00	34.84 ± 6.02	1,111.80 ± 77.02
14	38.78 ± 6.71	29.10 ± 6.74	0.00 ± 0.00	29.52 ± 5.59	151.64 ± 19.90
15	65.12 ± 6.25	42.15 ± 7.20	0.00 ± 0.00	0.00 ± 0.00	411.33 ± 62.05
16	27.23 ± 5.58	15.12 ± 3.55	0.00 ± 0.00	0.00 ± 0.00	492.35 ± 63.77
Median [IQR, cells/mm²]	**89.08 [45.37 - 306.37]**	**66.93 [24.20 - 235.74]**	**0.00 [0.00 - 0.00]**	**28.86 [0.00 - 50.64]**	**681.34 [459.87 - 1,000.33]**

Supplementary Table 3. Association between clinical features and tumour-infiltrating immune cells in 16 cats with appendicular osteosarcoma.

Clinical conditions	$CD3^+$ T cells		$CD8^+$ T cells		$Foxp3^+$ Tregs		$CD20^+$ B cells		$CD204^+$ macrophages	
	p value	Effect size (r/η^2 value)	*p* value	Effect size (r/η^2 value)	*p* value	Effect size (r/η^2 value)	*p* value	Effect size (r/η^2 value)	*p* value	Effect size (r/η^2 value)
Age[1]	0.0278*	-0.5856	0.0258*	-0.5918	0.3652	-0.2622	0.6342	-0.1396	0.9939	-0.0022
Body weight[1]	0.9643	-0.0132	0.7646	0.0881	0.2980	-0.2996	0.4599	-0.2153	0.6637	-0.1276
Sex[2]	0.5560	-0.0767	0.5030	0.0912	0.0806	0.3951	0.7284	-0.4796	0.7323	0.0669
Tumour location[2]	0.3189	0.1134	0.2458	0.2088	0.8908	-0.5679	0.8442	0.1034	0.2530	0.4583
Radiographic abnormality[2]	0.5152	-0.1627	0.6642	-0.1085	0.8504	-0.0471	0.3162	-0.2506	0.2781	-0.2712
Lameness[2]	0.5152	-0.1627	0.6642	-0.1085	0.8504	-0.0471	0.3162	-0.2506	0.2781	-0.2712
Metastasis at the time[2]	0.3855	-0.2169	0.5149	-0.1628	0.8504	-0.0471	1.0000	0.0000	0.1289	-0.3796
Lymph node metastasis[2]	0.1062	0.1912	0.1554	0.0207	0.7008	-0.1639	0.2671	0.1916	0.6065	-0.0479
Distant metastasis[2]	0.1262	0.1646	0.2595	-0.0372	0.2537	0.0785	0.4329	-0.0052	0.6639	0.0101
Local reccurence[2]	0.2628	0.0517	0.2466	0.0846	0.7818	-0.0991	0.4634	0.1319	0.5815	0.0377
Prognosis[2]	0.0137*	0.5057	0.0389*	-0.1454	0.5273	-0.4434	0.1201	0.2690	0.046*	0.2465
Survival time[1]	0.2493	-0.3059	0.1664	-0.3635	0.1670	-0.3630	0.1855	-0.3488	0.8882	-0.0382

[1] The data were analysed using Spearman's correlation Test; [2] The data were analysed using Kruskal–Wallis test; * $P < 0.05$.